

Substantial organic impurities at the surface of synthetic ammonium sulfate particles

Junteng Wu¹, Nicolas Brun¹, Juan Miguel González-Sánchez¹, Badr R'Mili¹, Brice Temime Roussel¹, Sylvain Ravier¹, Jean-Louis Clément², Anne Monod¹

5 ¹Aix Marseille Univ, CNRS, LCE, Marseille, France

²Aix Marseille Univ, CNRS, ICR, Marseille, France

Correspondence to: Junteng Wu (junteng.wu@univ-amu.fr) and Anne Monod (anne.monod@univ-amu.fr)

Abstract

Ammonium sulfate (AS) particles are widely used for studying the physical-chemistry processes of aerosols and for 10 instrument calibrations. Small quantities of organic matter can greatly influence the studied properties, as observed by many laboratory studies. In this work, monodisperse particles (~~from~~ 200 nm to 500 nm aerodynamic diameter) were generated by nebulizing various AS solutions and organic impurities were quantified relative to sulfate using a High-Resolution Time-of-Flight Aerosol Mass Spectrometer (HR-ToF-AMS). The organic content found in AS solutions was also tentatively identified 15 using a Liquid Chromatography–tandem Mass Spectrometry Spectrometer (LC-MS). The results from both analytical techniques were consistent and demonstrated that the organic impurities contained oxygen, nitrogen and/or sulfur, their molecular masses ranged from m/z 69 to 420, they likely originate from the commercial AS crystals. For AS particle sizes ranging from 200 nm to 500 nm, the total mass fraction of organic (relative to sulfate) ranged from 3.8 % to 1.5 ~~%%~~, 20 respectively. An inorganic-organic mixture model suggested that the organic impurities were coated on the AS particle with a surface ~~with a~~ density of $1.1 \times 10^{-3} \text{ g} \cdot \text{m}^{-2}$. A series of tests were performed to remove the organic content (using pure N₂ in the flow, ultrapure water in the solutions, and very high AS quality), showing that at least 40 % of the organic impurities could be removed. In conclusion, it is recommended to use AS seeds with caution, especially when small particles are used, in terms of AS purity and water purity when aqueous solutions are used for atomization.

1 Introduction

Atmospheric aerosols are generally a complex mixture of inorganic and organic compounds that have a strong impact 25 on climate and human health (IPCC, 2013; Pöschl and Shiraiwa, 2015). According to the annual aerosol emission inventories, inorganic compounds account for the majority of the mass (Andreae and Rosenfeld, 2008). Among them, ammonium sulfate (AS) is considered as one of the dominant components (Charlson et al., 1992; Seinfeld et al., 2016). Because AS plays important roles in physical and chemical atmospheric processes, it has been extensively used in laboratory experiments to understand and reproduce these processes. In the past 20 years, more than 200 articles have been published using AS as (seed)

30 particles for the study of optical properties, hygroscopic properties, phase transition and viscosity, as well as chemical reactivity of aerosols (see the detailed references in SI1). In all these studies, it was shown that the presence of organic matter, even at very low concentrations in AS particles, greatly influences these properties.

Among these, the study of aerosol hygroscopic properties represents the major contribution (115 papers out of the 263219 cited in SI1). AS aerosols are very often chosen as seed particles to study hygroscopic behavior of mixed organic-inorganic aerosols. Scanning various conditions of temperature and relative humidity (RH), hygroscopicity properties of aerosols were investigated via measurements of hygroscopic growth, cloud condensation nuclei (CCN) activity and ice nuclei (IN) activity. It is well ~~acknowledged established~~ that the hygroscopic parameter kappa (κ) of pure AS particles is 0.53 [0.33 - 0.72] and 0.61 according to the growth factor derivation and the CCN derivation, respectively (Clegg et al., 1998; Koehler et al., 2006; Petters and Kreidenweis, 2007). Laboratory studies show that the hygroscopic behavior of most water soluble inorganic mixed aerosols is additive in nature, i.e., following the ZSR (Zdanovskii, Stokes, and Robinson) assumption (Stokes and Robinson, 1966). However, when organic compounds are present in AS aerosols, their hygroscopic properties are more complex. Firstly, for water soluble organic compounds such as short carbon chain (di)carboxylic acids, their effects on AS aerosols are represented by their hygroscopicity and mass fraction suggested by the ZSR assumption (Abbatt et al., 2005; Brooks et al., 2004; Hämeri et al., 2002; Prenni et al., 2003). Secondly, for less soluble compounds and complex mixtures, 45 their solubility significantly influences the hygroscopic behavior of AS aerosol. At sub-saturation conditions, secondary organic aerosol (SOA) formed on AS seed particles from α -pinene photo-oxidation lowers the hygroscopic growth factor (HGF) of AS (Meyer et al., 2009). Specifically, at RH below the deliquescence point, AS seeded SOA do not follow the ZSR predictions ~~due to the incomplete dissolution because the solutions are highly concentrated and thus non-ideal~~. When the insoluble organic compounds are the dominant components of the aerosol, the water uptake on organic-AS particles is 50 significantly slowed down and requires a longer residence time to achieve the thermodynamic equilibrium (Sjogren et al., 2007). The same behavior has also been observed at super-saturation conditions, i.e., the thick coating of insoluble organics compounds such as stearic acids, act as a shield preventing the interaction of AS and water, thus suppressing AS hygroscopicity (Abbatt et al., 2005). Thirdly, ~~several studies have observed it was found~~ that ~~marine organics under low concentration and ozonolysis products of α pinene and monoterpane organic compounds could~~ affect AS's the hygroscopicity of AS by lowering 55 the surface tension, ~~thus enhancing their CCN activity (Engelhart et al., 2008; such as marine organic compounds at low concentrations (Moore et al., 2008), or ozonolysis products of monoterpenes (King et al., 2009; Moore et al., 2008; Wex et al., 2009; Engelhart et al., 2008)~~. It has been shown that atmospheric surfactants could reduce the aerosol surface tension by a factor of 2 compared to water surface tension ($72 \text{ mN}\cdot\text{m}^{-1}$) (Gérard et al., 2019; Nozière et al., 2014; Sorjamaa et al., 2004). The presence of ~~a~~ small amounts of surface-active organic compounds may reduce the aerosol surface tension, affecting its 60 hygroscopic properties: according to ~~recent some~~ models, a 10 % reduction of ~~10 % on~~ the surface tension results in ~~the a 30 %~~ increase of ~~30 % on~~ the hygroscopic parameter κ (Ovadnevaite et al., 2017; Petters and Kreidenweis, 2013). More recently, several models have shown that the inferred behavior of the surface tension strongly depends on the selected modelling

approach (Prisle, 2021; Vepsäläinen et al., 2022). In conclusion, organic compounds can have a very complex impact on the hygroscopic growth and CCN activity of aerosol particles which may go beyond the simple reduction of the value of a single parameter in the Köhler equation, and numerous models are currently under development on this issue.

AS has also been widely used to understand the phase transition of organic-inorganic compounds in single particles studies (49 papers out of the 263219 cited in SI1). Under sub-saturated conditions, deliquescence of pure AS occurs at ~ 80 % RH and efflorescence at ~ 34 % RH. However, these phase transition behaviors of AS particles are significantly influenced by organic compounds. For example, the presence of humic acids decreases the deliquescence RH and increases the efflorescence RH of AS aerosols (Badger et al., 2006). Furthermore, the presence of malonic acid on AS particle leads to a two-step deliquescence instead of a single step in the humidification process hygroscopic growth (Treuel et al., 2009). Differently to the shift of deliquescence RH and/or efflorescence RH, the presence of SOA completely removes the clear phase transition of AS on the particle: this was clearly shown for SOA derived from cycloalkene photolysis and monoterpenes photo-oxidation (Varutbangkul et al., 2006). The change in phase transition behavior of AS particle also depends on the quantity of organic compounds. In humidification process, During the hygroscopic growth, for small organic/inorganic ratios (< 20 %) lead %, there is a bulk-to internally mixing and/or surface partitioning with a part of the organic eating on material in solution, and another part as a film coated at the particle surface of the droplet (Nandy and Dutcher, 2018; Smith et al., 2013); while high organic/inorganic ratios (> 80 %) induce liquid-liquid phase separation (Smith et al., 2013; Saukko et al., 2015).

Due to their hygroscopic properties, AS aerosols easily provide an aqueous environment, where reactions between NH₄⁺, SO₄²⁻ and water-soluble organic compounds can play an important role on the formation of secondary aerosols (62 papers among the 263219 cited in SI1). Some of these reactions may explain the source of the so-called “brown carbon”, thus affecting the optical properties of particles (44 papers among the 263219 cited in SI1). Ammonium eatoncations (NH₄⁺) isare in a pH-dependent equilibrium with dissolved ammonia in the aqueous phase. NH₃ can react with carbonyl compounds such as glyoxal, methylglyoxal, glycolaldehyde, hydroxyacetone, biacetyl or unsaturated dialdehydes in Maillard-type browning reactions to form light absorbing and oligomeric compounds such as imidazoles or pyrazine-based compounds (Hensley et al., 2021; Grace et al., 2020; Hawkins et al., 2018; Laskin et al., 2014; Kampf et al., 2012). These reactions are of particular interest for the atmosphere, as they have an impact on both health and climate. Their aqueous-phase processes represent an important and rapid source of brown carbon (Powelson et al., 2014; De Haan et al., 2017; Jimenez et al., 2022). In addition, SO₄²⁻ is not inert in atmospheric water. Aqueous phase reactions Sulfate anions can react with isoprene derived epoxides to form organo sulfates have been reported (Darer et al., 2011; Liggi OH radicals forming sulfate radicals (SO₄²⁻), an important atmospheric oxidant (Herrmann, 2003). Besides, sulfate radicals contribute to the formation of organosulfates (Nozière et al., 2005). Epoxides, which 2010; Brüggemann et al., 2020; Wach et al., 2019; Szmigielski, 2016). Organosulfates are formed by the ozonolysis of a carbon-carbon double bond, undergo an acid catalyzed nucleophilic attack by sulfate anions. In addition, tertiary organic nitrates, formed by nighttime NO₃ reaction ubiquitous compounds in SOA with isoprene or other terpenes, undergo important implications in their physicochemical properties (Shakya and Peltier, 2015). Other chemical pathways that lead to the formation of organosulfates might involve directly sulfate anions, i.e., their nucleophilic substitution in the presence

~~of sulfates forming organo-sulfates to epoxides or tertiary nitrates (Hu et al., 2011; Darer et al., 2011), and the acid-catalyzed esterification of alcohol groups (Surratt et al., 2008; Jinuma et al., 2007).~~

Due to the atmospheric representativity of AS particles and their well-known physical and chemical properties, they are often chosen as a reference in aerosol studies, as mentioned above, and for instrumentation calibration. The presence of trace organic compounds in AS particles may induce potentially important artefacts on the experimental results of physical and chemical processes. Few laboratory studies show that organic compounds can be present in synthetic AS particles. For example, 0.8 wt % of C was observed in solutions where only ammonium sulfate ~~solutions was present as solute~~ in the study of phase transitions of AS ~~and humic acid mixtures (Badger et al., 2006)~~. Another example, in a study of glyoxal uptake on AS particles monitored by an Aerosol Mass Spectrometer, ~~Trainic et al., 2011~~ Trainic et al., (2011) found organic fragments on pure AS aerosols (purity not mentioned), with an organic/sulfate ratio as high as 8 ~~—~~ %. Scanning the ~~263~~ 219 articles (mentioned in SI1) published over the last 20 years using AS aerosols in the laboratory, it appeared that neither quantification nor identification of these potential organic impurities was reported. Furthermore, the majority of these studies (~~62~~ 63 %) did not mention the origin and purity of AS used. As organic traces may significantly influence the properties of AS particles, and thus bias experimental results, the objectives of this work were to quantify organic traces in commercial AS under conditions used in laboratory experiments, and when possible, tentative identification was performed, ~~and finally~~. Finally, recommendations are given for purity improvements.

2 Method

AS ~~suspended aerosol~~ particles were generated by atomization of AS solutions at concentrations ranging from 0.01 to 0.5 M, ~~similar to those previously employed.~~ AS aerosols were selected at 4 sub-micrometer sizes to test the effect of particle size on the organic content. This procedure allowed us to form quasi-monodisperse AS particles at mass concentrations ranging from 5 to 30 $\mu\text{g m}^{-3}$, ~~similar to those previously employed concentrations typically used for aerosol generation and/or calibration in the literature.~~ Their chemical composition was quantified on-line by a high-resolution time-of-flight aerosol mass spectrometer (HR-ToF-AMS). ~~In parallel~~ Additionally, aqueous solutions of AS were ~~prepared and~~ analyzed by ~~a~~ Liquid Chromatography–tandem Mass Spectrometry (LC-MS) to tentatively identify organic content. All chemical compounds used in this work are listed in SI2.

2.1 Detection of organic traces in AS ~~suspended aerosol~~ particles

2.1.1 Aerosol generation and size classification

~~A scheme~~ The schematic of the experimental setup for quantifying organic content is shown in ~~Figure 4~~ Fig. 1. Aqueous solutions of AS (0.01 - 0.5 M) were nebulized by atomization (using a TSI, 3076 atomizer) that generated droplets with compressed air at 1 bar above atmospheric pressure and a flowrate of 1.8 L min^{-1} . As a comparison with compressed air, pure N₂ (Linde Gas, 99.999 %) was used. The resulting droplets were dried by a NafionTM dryer at relative humidity (RH)

below 25 %, i.e., below the efflorescence of AS aerosol. Dry AS particles then passed through a dilution system aimed at controlling AS particle concentrations. It consisted ~~in~~ of two parallel pathways, one of which was connected to a HEPA filter. 130 An aerodynamic aerosol classifier (AAC, Cambustion) and an electrostatic classifier (TSI, 3080) combined with a differential mobility analyzer (3081 long DMA, TSI, 3080) were alternatively used to select monodisperse particles. The sheath/sample air flow ratio was fixed at 10 for the two classifiers. To regulate the flowrate ~~at~~through the ~~exhaust~~AAC classifier, a mass flow controller (MFC) was connected to a vacuum pump. Under this configuration, the sample flow ~~before~~through the classifierAAC varied from 0.4 to 1.4 L min⁻¹, while the tests performed with the DMA classifier were only done at one flowrate 135 (0.4 L min⁻¹). This setup allowed the characterization of the suspended aerosol particles by their mobility, aerodynamic and vacuum aerodynamic sizes, as well as their organic content as a function of particle sizes with respect to the total mass of AS particles selected.

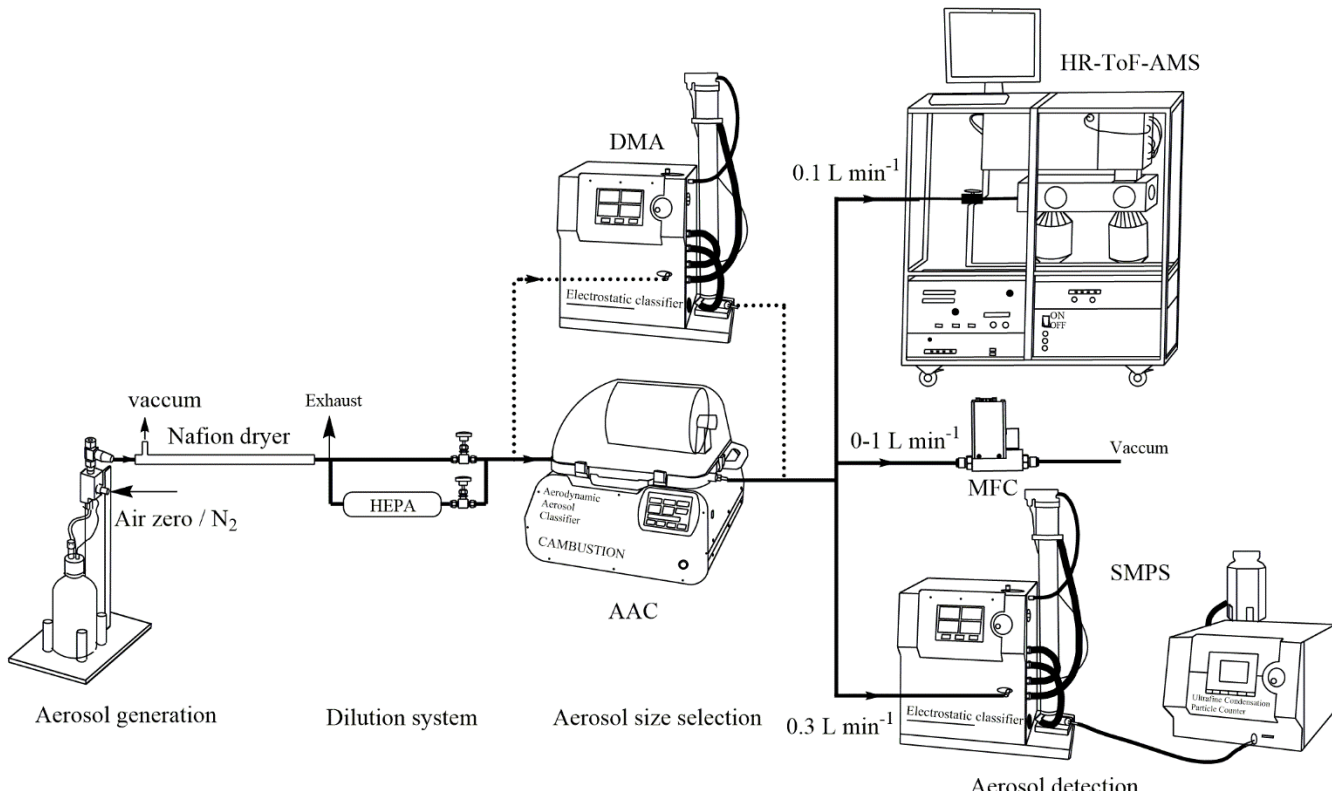


Figure 1. Experimental setup for the quantification of organic content in monodisperse ammonium sulfate particles.

140 **2.1.2 Experimental conditions for the investigation of AS suspended aerosol particles**

A series of experiments (Table 1) was performed to quantify organic content on suspended AS aerosol particles by scanning various conditions of mass concentrations, particle size, and generation procedures. In this work, four different particle diameters were used: the mobility diameter (d_m), the aerodynamic diameter (d_a), and the vacuum aerodynamic diameter

(d_{va}) were given by the SMPS, the AAC and the AMS measurements, respectively; while the volume equivalent diameter (d_{ve}) was used to determine the surface of AS particle. The relations between these diameters were described by DeCarlo et al., (2004). As organic compounds can be homogenously mixed in AS aerosol or remain at particle surface inducing different behavior as a function of size (Jimenez et al., 2009; Tervahattu et al., 2002), monodisperse AS particles were selected with aerodynamic size (d_a) varied from 200 nm to 500 nm in each experiment. In experiment P1 (EXP P1), AS crystals (99.5 %, for analysis, from ACROS Organics™ Fisher Scientific) were dissolved in Milli-Q water ($18.2 \text{ M}\Omega\text{-cm}^{-1}$, TOC $< 2 \text{ ppb}$) at various concentrations (0.01 - 0.5 M). In EXP P2 to P7, the aqueous phase concentration of AS was fixed at the highest value (0.5 M) to study the influence of other parameters. In EXP P2, the influence of the water quality was tested. In EXP P3 to P5, the influence of the purity of AS crystals was tested. In EXP P3, AS crystals (99.5 %, for analysis, from ACROS Organics™ Fisher Scientific) were tentatively purified by an Accelerated Solvent Extractor (ASE 300, Dionex) using acetonitrile as extraction solvent. In EXP P4, AS crystals (99.5 %, for analysis, from ACROS Organics™ Fisher Scientific) were tentatively purified by recrystallization in Milli-Q water: AS crystals (20 g) were dissolved into boiling water (20 mL) reaching a concentration of 7.5 M and then recrystallized by smooth cooling at room temperature. In EXP P5, high purity AS (99.9999% Suprapur® from Merck) was used. In EXP P6, the influence of the particle size selector was studied by inter-comparison between the DMA and the AAC. Developed by Tavakoli and Olfert (2013), the AAC is a recent commercial aerosol classifier which selects the particle size by centrifugal force instead of electrostatic force which is used in the DMA. In the AAC, the aerodynamic diameter of selected particles is related to the rotational speed of the concentric cylinder, the sheath flow rate and the sample flow rate. Rotational speed has been reported to influence the geometric standard deviation (δ_{geo}) of size distribution, i.e., the smaller size, the higher the rotational speed, the smaller the size and the larger the δ_{geo} (Johnson et al., 2018). In EXP P7, the effect of the rotational speed of the concentric cylinder in the AAC was tested while maintaining a constant size selection by regulating the MFC (Figure Fig. 1), so that the sample flow through the AAC varied from 0.4 to 1.4 $\text{L}\text{-min}^{-1}$.

Table 1. Experiments to quantify organic traces on suspended AS aerosol particles under various conditions: ⁽¹⁾ AS 99.5%, for analysis, from ACROS Organics™ Fisher Scientific; ⁽²⁾ purification by solvent (acetonitrile) extraction; ⁽³⁾ purification by recrystallisation; ⁽⁴⁾ AS 99.9999% Suprapur® from Merck. ⁽⁵⁾ Milli-Q water, $18.2 \text{ M}\Omega\text{-cm}^{-1}$, TOC $< 2 \text{ ppb}$; ⁽⁶⁾ Fisher Chemical, LC-MS Grade. Under each condition, duplicate experiments were performed for each selected particle size. The four sizes ($d_a = 200, 300, 400$ and 500 nm) selected with the AAC classifier correspond to the mobility sizes ($d_m = 130, 201, 269$ and 336 nm)

Experiment	AS purity %	water	AS liquid concentration (M)	Particle size (nm)
Size selection by the AAC (sample flow = $0.4 \text{ L}\text{-min}^{-1}$)				
P1	99.5 ⁽¹⁾	Milli-Q ⁽⁵⁾	0.01, 0.02, 0.05, 0.1, 0.2, 0.5	$d_a = 200, 300, 400, 500$
P2	99.5 ⁽¹⁾	Fisher ⁽⁶⁾	0.5	$d_a = 200, 300, 400, 500$
P3	99.5 ⁽¹⁾ purified ⁽²⁾	Fisher ⁽⁶⁾	0.5	$d_a = 200, 300, 400, 500$
P4	99.5 ⁽¹⁾ recryst ⁽³⁾	Fisher ⁽⁶⁾	0.5	$d_a = 200, 300, 400, 500$

P5	99.9999 ⁽⁴⁾	Fisher ⁽⁶⁾	0.5	$d_a = 200, 300, 400, 500$
Size selection by the DMA (sample flow = 0.4 L.min ⁻¹)				
P6	99.5 ⁽¹⁾	Milli-Q ⁽⁵⁾	0.5	$d_m = 122, 188, 250, 311, 375$
Size selection by the AAC (sample flow = 0.5, 1.0, 1.4 L.min ⁻¹ , corresponding to rotation speed of 190, 285 and 369 rad/s)				
P7	99.5 ⁽¹⁾	Milli-Q ⁽⁵⁾	0.5	$d_a = 300$
<u>Effect of gas supplier (pure N₂ instead of compressed air)</u>				
P8	<u>99.5 ⁽¹⁾</u>	<u>Milli-Q ⁽⁵⁾</u>	<u>0.5</u>	<u>$d_a = 200, 300, 400, 500$</u>

2.1.3 Characterization of suspended aerosol particles

The particles number size distribution was measured with a scanning mobility particle sizer (SMPS) consisting of a

175 Differential Mobility Analyzer (DMA, DMA (TSI, 3080) coupled with an Ultrafine Condensation Particle Counter (CPC, 3776, TSI). A high-resolution time-of-flight aerosol mass spectrometer (HR-ToF-AMS, Aerodyne Research) was used to measure the bulk chemical composition of non-refractory submicron particulate matter (DeCarlo et al., 2006). The instrument was used under standard conditions (standard vaporizer at 600 – 650 °C and electron ionization at 70 eV) in V-mode and in p-
180 ToF mode. Each measurement point was averaged for MS cycle of 1 min and p-ToF cycle of 30 s. Calibrations with using pure and dried particles of ammonium nitrate and ammonium sulfate with a mobility diameter of 350 nm was carried out every few days of operation to determine the Ionization Efficiency of nitrate, ammonium and sulfate named as IE_{NO3}, RIE_{NH4} and RIE_{SO4}. The RIE_{NH4} and RIE_{SO4} values obtainedwere related to nitrate and were estimated experimentally areas 3.3 and 1.8, respectively. The standard recommended value for RIE_{org} of 1.4 was used for organicsorganic compounds. Calibration in p-
185 ToF mode was carried out using pure ammonium nitrate in the size range 80-500 nm mobility diameter. The data treatment has been performed bywith AMS Analysis Toolkit 1.63 and PIKA 1.23 under the software Igor Pro 6.37. The selection of ions to fit in PIKA was derived from the mass spectra produced by AS aerosols at $d_a = 200$ nm in EXP P1 and was re-checked in each experiment. The measured mass spectra were dominated by NH_x and SO_x fragments, but air fragments such as N⁺, O⁺, HO⁺, H₂O⁺, N²⁺, ¹⁵NN⁺, O²⁺, ¹⁸OO⁺, Ar⁺, CO²⁺ showed also large ion signals. To avoid any over-estimation of the organic fraction, only CHO⁺ and CO₂⁺ were apportioned to organics using C₂H₃O⁺ followingfragments (at m/z 29 and 44) were corrected from the procedure of remaining gas phase in the AMS (Aiken et al., (2007) and Canagaratna et al., (2015)). In addition, due to the very high signals of the fragments NH_x and SO_x, other fragments located at the tail of these main peaks (such as CH₃⁺, CH₄⁺, CH₂N⁺ and C₂H₄⁺...) were excluded from the calculation of the total organic content, to avoid any over-estimation of the organic fraction.

195 **2.2 Seeking for organic traces in AS aqueous solutions**

In parallel with the The characterization of suspended AS particles, organic traces on AS aerosol particles were also investigated directly in AS aqueous solutions by using a Liquid Chromatography–tandem Mass SpectrometrySpectrometer (LC-MS) for tentative molecular identification. The system comprised liquid chromatographychromatograph (Acquity system, Waters) coupled with Quadrupole-Time-of-Flight Mass SpectrometrySpectrometer (Synapt G2 HDMS, Waters) fitted with an electrospray ion source (ESI). The chromatographic separation was carried out on an Atlantis T3 reversed phase C18 column (100*2.1; 3 μ m, Waters), the mobile phase consisted in of two eluents: eluent A was Milli-Q water (resistivity 18 $M\Omega\text{-cm}^{-1}$ at 25 °C) with 0.1 % formic acid, and eluent B was either methanol (Optima[®] LC/MS grade, Fisher Scientific) with 0.1 % formic acid or acetonitrile (Fisher Chemical, Optima[®] LC/MS grade) with 0.1 % acid. The gradient elution was performed at a flow rate of 0.4 mL min⁻¹ using 5 % of (B) held 1 min and 5 – 95 % of (B) within 5 min. The sample injection volume was 5 μ L. In 200 the ESI, the capillary voltage was set to 1 kV, the desolvation gas flow was 1000 L -h^{-1} at 500 °C and the source temperature was 150 °C. During each chromatographic run, leucine enkephalin (2 ng $\text{-}\mu\text{L}^{-1}$, C₂₈H₃₇N₅O₇, molecular weight 555.27 g $\text{-}\text{mol}^{-1}$, Sigma-Aldrich) was used as internal standard to perform mass correction. The mass spectrometer was tuned to V-mode with 205 a resolving power of 18-00018000 at m/z 400 and allowed the determination of elemental composition with a mass accuracy lower than 5 ppm. For elemental attribution, the ranges of atom number were set as follows: C [0-30], H [0-60], N [0-5], O [0-10], S [0-3], P [0-3], Na [0-1] thus covering the most common elements (Kind and Fiehn, 2007)(Kind and Fiehn, 2007). An 210 isotope prediction algorithm, based on the mass of the molecular ion and the relative intensity of the 1st and 2nd isotopes, was applied to reduce the number of proposed elemental compositions. Data were collected from 50 to 600 Da in the positive and negative ionization modes. All products were detected as their protonated molecules ([M+H]⁺) or sodium adducts ([M+Na]⁺) in the positive mode, and their deprotonated molecules ([M-H]⁻) in the negative mode. In some experiments, complementary 215 analyses were performed using MS/MS fragmentation with various collision energies.

Although the organic purity is not mentioned on commercial crystals (only the inorganic content is indicated), two different brands of AS of the same purity were analyzed to seek for potential organic traces and for comparison purposes: one from ACROS OrganicsTM Fisher Scientific (99.5 %, for analysis) that has been widely used in the literature and one EMSURE[®] from Merck (99.5 %, for analysis). The characterization experiments are shown in Table 2, each one was systematically 220 complemented by blank experiments, i.e., analysis of the water used for each AS solution.

225 Table 2: Experiments of characterization of organic traces in AS liquid solutions. The elution gradient and ESI setup were the same for all experiments. ⁽¹⁾ AS 99.5%, for analysis, from ACROS OrganicsTM Fisher Scientific; ⁽²⁾ AS 99.5% EMSURE[®] from MERCK ⁽³⁾ Eluents: A=H₂O with 0.1% formic acid, and B as specified; ⁽⁴⁾ acetonitrile, ⁽⁵⁾ methanol, ⁽⁶⁾ methyl tert-butyl ether, ⁽⁷⁾ dichloromethane. L-L: liquid-liquid, S-L: solid-liquid.

Experiment	Type of experiment	LC-MS analytical conditions
------------	--------------------	-----------------------------

	AS purity %	AS aqueous concentration	Sample preparation	Extracting solvent	Eluent B ⁽³⁾	MS Mode	
C1	99.5 ⁽¹⁾	1.5 M	No (direct injection) <u>N</u> one	-	ACN ⁽⁴⁾ 0.1% acid	ESI⁺-MS/ ESI-MS	
C2					MeOH ⁽⁵⁾ 0.1% acid		
C3				L-L extraction	MTBE ⁽⁶⁾	ESI⁺-MS / ESI-MS	
C4					DCM ⁽⁷⁾		
C5					ACN ⁽⁴⁾ 0.1% acid		
C6		2.5 M		S-L extraction	ACN ⁽⁴⁾	ESI⁺-MS-MS	
C7							
C8	99.5 ⁽²⁾	crystals					
C9	99.5 ⁽¹⁾	L-L extraction		MeOH ⁽⁵⁾ 0.1% acid	ESI⁺-MS / ESI-MS		
C10	99.5 ⁽²⁾					5 M	

In EXP C1 and C2, aqueous solutions of AS were ~~directly~~ injected into the LC-MS, and two elution solvents were tested to optimize the chromatographic separation, ~~the signal was only monitored in ESI⁺.~~ In EXP C3 to C10, organic compounds were extracted from AS crystals by different methods (solid-liquid and liquid-liquid extraction) using various solvents, and preconcentrated prior LC-MS analysis using both positive and negative modes. For these extractions, an Accelerated Solvent Extractor (ASE 300, Dionex) system was used under the following conditions: acetonitrile was the extraction solvent, the oven was set at 100 °C under 100 bars, the heat up time and static time were 5 min each, three extraction cycles were ~~operated conducted~~. As an extension of EXP C6, EXP C9 was designed to perform MS/MS analysis using very high concentrations of AS to optimize the identification of organic traces, and analysis were performed in the positive mode only. For comparison purposes, another brand of AS of the same purity (99.5 %) were used in EXP C8 and C10 using two extraction methods.

3 Results and discussions

3.1 Organic content on AS ~~suspended aerosol~~ particles

A significant quantity of organic matter was directly observed by the HR-ToF-AMS in EXP P1. As an example, Figure 2 shows the mass concentrations of total organic matter and sulfate and their ratios as a function of time during one size

cycle performed in EXP P1 at AS concentration of 0.01 M. Figure 2 also provides background signals obtained with the two pure waters ~~in~~ of different qualities used in EXP P1 and P2. In these background signals, the total mass concentrations of ~~organics~~organic compounds and sulfate are $0.018 \pm 0.009 \mu\text{g m}^{-3}$ and $0.002 \pm 0.001 \mu\text{g m}^{-3}$ respectively, similar to the detection limits of the HR-ToF-AMS in the V mode (DeCarlo et al., 2006). In the presence of AS, a significant quantity of ~~organics~~organic compounds was observed with concentrations ranging from 0.15 to $0.33 \mu\text{g m}^{-3}$ when aerodynamic size of the particle varied from 500 nm to 200 nm, with a very good reproducibility in the duplicate experiments, at each size. Furthermore, the evolution of the mass ratio between total organic compounds and sulfate marked as $[\text{Org}]/[\text{Sulfate}]$ (Fig. 2) shows a clear correlation with particle size: this ratio increases when the particle size decreases. The same observations were ~~made obtained~~ at all other AS concentrations investigated in EXP P1 and in the other experiments. It was checked in EXP P8 that replacing compressed air by pure N2 (Linde Gas, 99.999 %), no significant differences were observed from EXP P1 under the same conditions (SI3). Overall, it was observed that $[\text{Org}]/[\text{Sulfate}]$ varied from 1.5 % to 3.8 %, ~~respectively~~ slightly higher (respectively lower) than in the two previous ~~in the range of the values reported by~~ studies mentioning the presence of organic compounds in laboratory experiments on AS particles (~~respectively~~ 0.8 wt % of C in Badger et al., 2006 and up to 8% in Trainic et al., 2011).

255

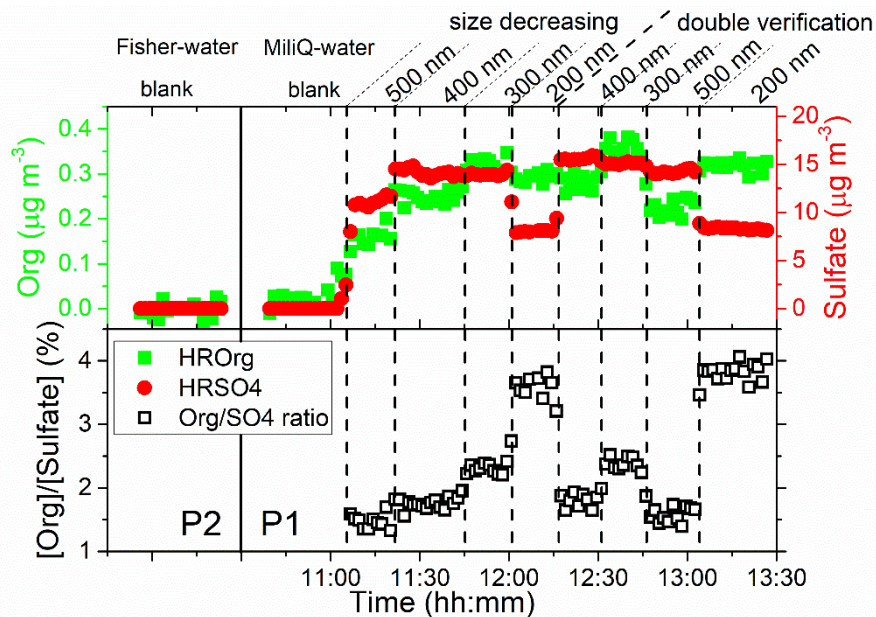


Figure 2: Mass concentrations of total organic matter, sulfate and organic/sulfate ratio as a function of time during one cycle performed in EXP P1 at AS concentration of 0.01 M. Background signal obtained with pure water in EXP P1 and P2 is also shown for quality check and for comparison between the two ~~pure waters in~~ types of water with different ~~qualities~~ purity.

The total mass concentration of organic compounds was calculated based on all organic fragments, as described in the previous Sect 2.1.3. Figure 4-3 shows the Unit-mass **HR ToF AMSresolution** spectrum of AS aerosols selected by the AAC at $d_a = 200$ nm.

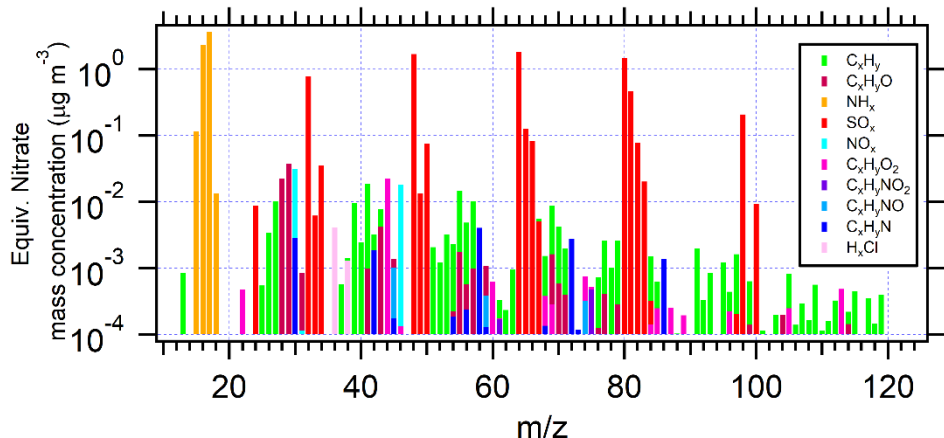


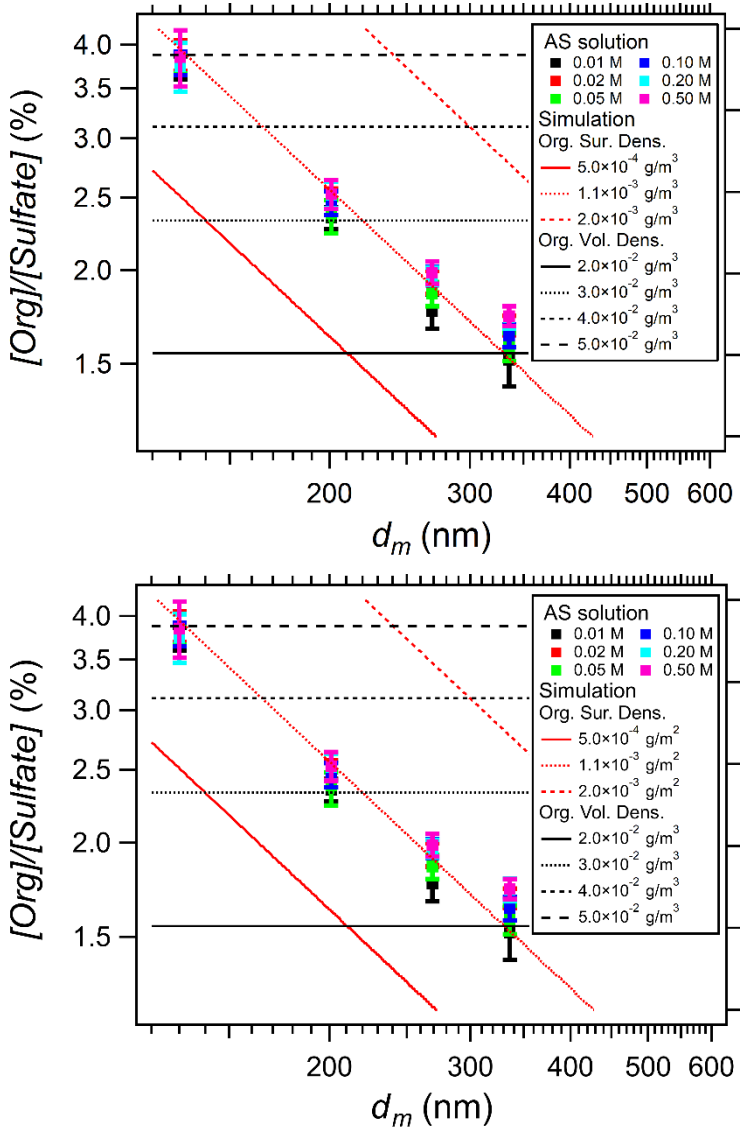
Figure 3 : Unit-mass **resolution** spectra (averaged over 12 **measurements**, converted from the high-resolution data) of AS suspended **aerosol** particles ($d_a = 200$ nm) in EXP P1, performed at AS concentration of 0.5 M.

Representing **SO_x** and **NH_x** families represent sulfate and ammonium, respectively. **SO_x⁺** and **NH_x⁺** are the major fragments. All the other fragments are between 1 and 3 orders of magnitude lower, but detectable signals span for m/z up to 100. The low signal detected for the **NO⁺** and **NO₂⁺** fragments at m/z 30 and 46, inhibits the distinction between inorganic and organic nitrate. The sum of the signals of **NO₂⁺** and **NO⁺** fragments represent 30% of the total organic signal (Fig. SI4-2). To figure out the source of this non-negligible nitrate signal, the AMS signal **NO₂⁺/NO⁺** ratio was investigated and showed significantly lower values in AS aerosol (0.46 in EXP1) compared to ammonium nitrate particles used for calibration (1.18) – Fig. SI4-1. It is thus suggested that the observed nitrate signal in AS aerosol is due to the presence of organic nitrates (Kiendler-Scharr et al., 2016). Concerning organic fragments, significant signals were observed for fragments **C_xH_y⁺** at m/z 27, 39, 41, 43, 55, 57, 67, 69, for **C_xH_yO⁺** at m/z of 28 and 30, for **C_xH_yO₂⁺** at m/z 44, for **C_xH_yN⁺** at m/z 30, 58, 72, 86 (raw spectra of CHN fragments are shown in SI3). These signals seem to represent large SI5. The potential “Pieber effect” was also investigated to elucidate any positive artefact on the determined quantities of organic compounds. Indeed, Pieber et al., 2016 showed that inorganic salts like AS or ammonium nitrate can trigger the **CO₂⁺** signal (m/z 44) due to reactions on the vaporizer of the AMS instrument. In the present study, the observed **CO₂⁺** signal represented 20 ± 5 % of the total organic signal. Thus, if all the **CO₂⁺** fragments came from the interference signal of sulfate, the maximum Pieber effect in this work would be 0.76 % relative to sulfate. It was thus not considered in the results. The rest of the organic fragments seem to represent organic molecules bearing various functionalities, potentially comprising oxygen and nitrogen. Before further identification of these compounds, Sect 3.2 and Sect 3.3 present the results and discussions on the influence of the particle size and liquid AS concentrations on the organic content.

3.2 The role of particle size and liquid AS concentrations on the quantity of organic content

285

Figure 4 shows the [Org]/[Sulfate] measured in AS aerosols at various nebulized solution concentrations as a function of particle size. While no significant influence of AS aqueous phase concentration has been found (within experimental uncertainty), a significant influence of particle size is clearly observed on the [Org]/[Sulfate].



290

Figure 4 : Organic/sulfate mass concentration ratios in AS aerosols versus particle mobility size (d_m) during EXP P1 scanning the six nebulized AS concentrations (0.01 to 0.5 M). The colored dots (with error bars) are the experimental data, while the red and black lines represent the calculated [Org]/[Sulfate] considering either surface coating of organic matter (in red from Eq. 3) or internal mixing (in black from Eq. 4).

To further understand how the organic matter was mixed with AS aerosols, two series of calculations were performed,

following two ~~hypothesizes~~ on the organic-inorganic mixing: i) organic coating on the surface of monodisperse AS particles, and ii) internal mixing. To achieve this calculation, a thorough study of the morphology of AS particles was ~~needed which was obtained from multi-characterization of particle size performed using the various sizes measurements (Appendix A)~~. For monodisperse AS particles selected by the AAC at a required aerodynamic diameter (d_a), its mobility diameter (d_m) and vacuum aerodynamic diameter (d_{va}) were measured by SMPS and HR-ToF-AMS, respectively.

The calculations ~~performed under of the organic-sulfate ratio using~~ each of ~~the~~ these two ~~hypothesizes on the organic-inorganic mixing~~ are detailed hereafter:

- Hypothesis 1: AS aerosols were coated by organic compounds with a size-independent ~~surface~~ density $\rho_{org,S}$ (in $\text{g}\cdot\text{m}^{-2}$).

For non-spherical particle, the total surface of particle was considered as the surface of volume equivalent particle. ~~According to DeCarlo et al., (2004), the relation between volume equivalent diameter (d_{ve}) and d_a is determined in Appendix A. According to DeCarlo et al., (2004), the relation between volume equivalent diameter (d_{ve}) and d_a is described as Eq. 1:~~

$$d_a = d_{ve} \sqrt{\frac{\rho_p}{\rho_0} \frac{1}{\chi} \frac{C_c(d_{ve})}{C_c(d_a)}} \quad (1)$$

Where χ is the shape factor of aerosol particles and C_c is the Cunningham slip factor (~~Kim et al., 2005~~) (~~Kim et al., 2005~~), given by Eq. 2.

$$C_c(K_n) = 1 + K_n \left[1.165 + 0.483 \exp \left(-\frac{0.997}{K_n} \right) \right] \quad (2)$$

$K_n(d) = 2\lambda_g/d$ is the Knudsen number, and λ_g is the gas mean free path. In this work, ~~normal d_a was given by the AAC; χ was determined by d_m and d_{va} (Appendix A). Normal~~ temperature and pressure (293.15 K at 1 atm) were applied for the calculation of ~~the shape factor of AS aerosols. In this work, morphological properties d_{ve} . The surface of AS particles are shown in Appendix A: Morphological properties of AS aerosols was estimated from the value of d_{ve} .~~ Therefore, the prediction of surface coated organic compounds compared to sulfate mass is described in Eq. 3.

$$\frac{[\text{Org}]}{[\text{Sulfate}]} = \frac{\rho_{org,S} S_{ve}}{V_{ve} \rho_{AS} \frac{M_{SO_4}}{M_{AS}}} = \frac{3}{2} \frac{\rho_{org,S}}{d_{ve} \rho_{AS} \frac{M_{SO_4}}{M_{AS}}} \times 100\% \quad (3)$$

Where S_{ve} and V_{ve} are ~~respectively~~ the surface and volume of the volume equivalent AS particle, ~~respectively~~. M_{SO_4} and M_{AS} are molar mass of SO_4^{2-} and $(\text{NH}_4)_2\text{SO}_4$, respectively. $[\text{Org}]$ and $[\text{Sulfate}]$ are the mass concentrations of organic compounds and of sulfate in the particulate phase. Eq. 3 shows that, in this case, the ratio $[\text{Org}]/[\text{Sulfate}]$ decreases when the particle size increases.

- Hypothesis 2: Organic compounds are homogeneously mixed in AS aerosols with an density $\rho_{org,V}$ (in $\text{g}\cdot\text{m}^{-3}$).

In this case, the mass concentrations of organic compounds compared to sulfate is described by Eq. 4.

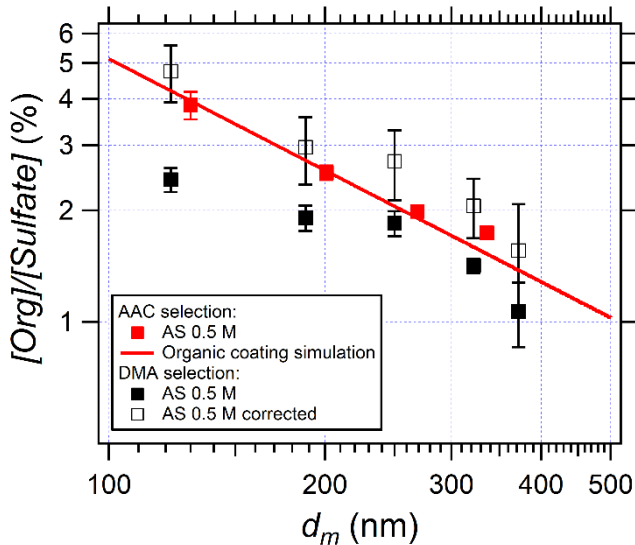
$$\frac{[Org]}{[Sulfate]} = \frac{\frac{\rho_{org,V}V}{M_{SO_4}}}{\frac{V\rho_{AS}M_{AS}}{M_{SO_4}}V\rho_{AS}} = \frac{\frac{\rho_{org,V}}{\rho_{AS}M_{AS}}}{\frac{M_{SO_4}}{M_{AS}}\rho_{AS}} \times 100\% \quad (4)$$

Where V is the total volume of studied aerosol particle. In this case, the ratio $[Org]/[Sulfate]$ is independent ~~to~~ of the particle size.

325 The results of these two calculations are shown in Fig. 4 together with the experimental results. The comparison clearly shows that the organic compounds coat homogenously on the surface of AS particles with a surface density of 1.1×10^{-3} g \cdot m $^{-2}$. In addition, this result also shows that the NafionTM dryer ~~is~~ was not efficient in removing these organic compounds, probably due to their low volatility.

330 3.3 Influence of AAC and DMA on the organic content

Particle size selection is important in aerosol science especially when particle size influences the properties studied. In this work, both AAC and DMA were used to provide monodisperse AS aerosols. As a recent commercial instrument, AAC was used to select AS aerosols in most of the experiments. The effects of the concentric cylinder rotation speed of the AAC were tested in EXP P7. The results ([SI4](#)[SI6](#)) demonstrate that the rotation speed does not affect the $[Org]/[Sulfate]$. While the 335 AAC selects particles using centrifugal force, the DMA selects particles ~~bearing a given electrical mobility size, providing size distributions that are by their electromobility. In the latter, the selected distribution is thus not perfectly monodisperse but with exclusively monodispersed as it contains double or and triple modes, due to charged particles at the corresponding sizes. Corrections of the multi-charging effects. DMA has been widely used so corrections of these effects have been charge effect were~~ successfully applied ~~following the and is routine~~ in aerosol ~~studiessize~~ distribution determination (Petters, 2018; 340 Wiedensohler et al., 2012). ~~However, Figure 4 shows that the larger particle the lower content of the organic compounds. In this case, the multi-charged particles affect the organic quantification using the DMA and the AMS, so that corrections are needed to do.~~ In this work, we compared $[Org]/[Sulfate]$ in AS particles selected by the DMA and by the AAC, respectively ([Figure](#) [Fig.](#) 5).



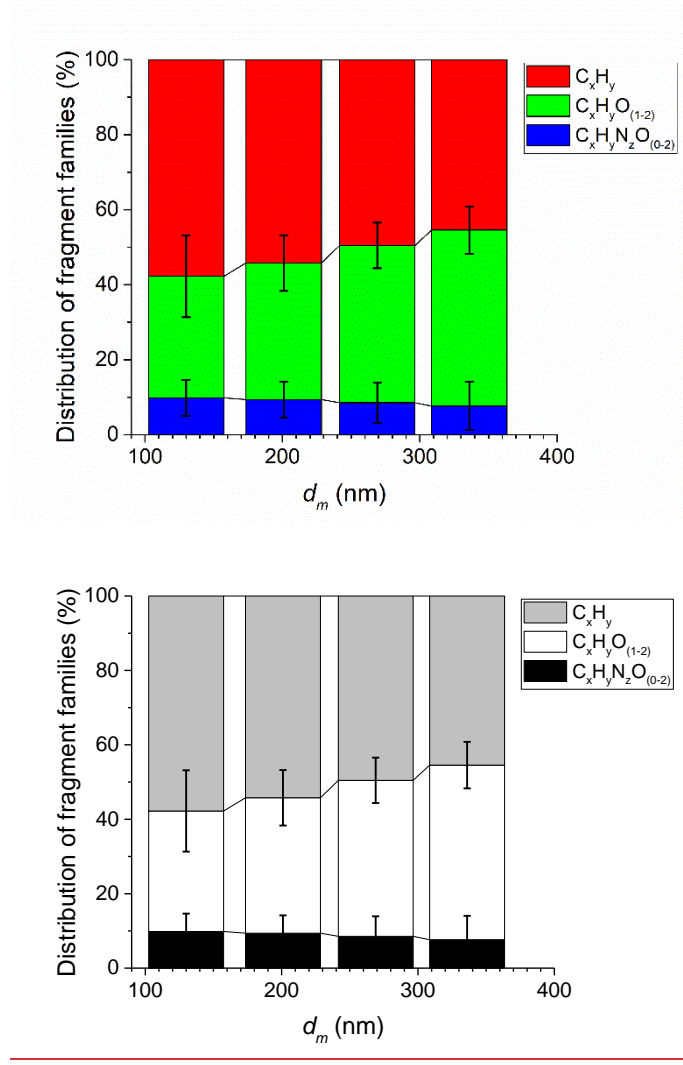
345

Figure 5 : Influence of instrumental conditions and instrument inter-comparison: AAC selection (red squares, EXP P1), DMA selection (black squares, EXP P6) and multi-charging correction (white squares). The red line represents the calculation simulating organic coated at the AS particle surface using Eq. 3 with a surface density of 1.1×10^{-3} g·m⁻² (selected from Fig. 4).

350 The white squares represent the multi-charging corrections considering the hypothesis that organic compounds coat the surface of AS particles as shown in Sect 3.2. Details of the multi-charging corrections are given in [SI5SI7](#). Briefly, the corrected [Org]/[Sulfate] by the multi-charged modes are systematically higher than the non-corrected values because the correction considers the total amounts of [organics](#)[organic compounds](#) and sulfate. [From the results, using](#)[Using](#) the DMA selection after correction, the [Org]/[Sulfate] is clearly inversely related to the mobility size and in very good agreement with those obtained using the AAC selection. In conclusion, the intercomparison of the two instruments shows that the influence of 355 the instrument is negligible, and it also shows that the selection by AAC leads to lower uncertainties [on the y axis](#) and therefore more accurate results.

3.4 Tentative Identification of organic content

360 From the HR-ToF-AMS mass spectra, the three main [organic fragments](#)[families](#) present in AS particles were C_xH_y, C_xH_yO₍₁₋₂₎ and C_xH_yNO₍₀₋₂₎. Figure 6 shows the proportion of these three groups relative to total [organics](#)[organic compounds](#) as a function of AS particle size. Within the uncertainties, the proportion of the three families remains constant and independent on the particle size, which shows the stability of the organic compounds coated on AS particles.



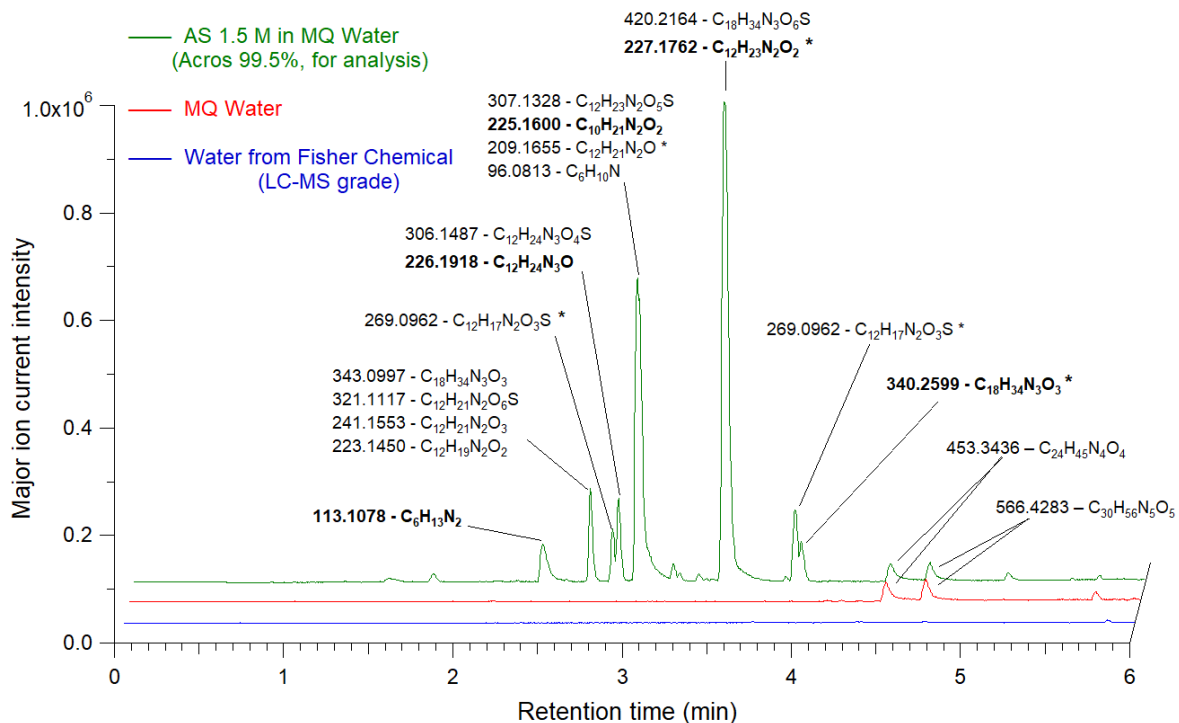
365 **Figure 6:** Mass fractions of the three main sets of organic fragments present in AS particles as measured by the HR-ToF-AMS during EXP P1. The error bars represent the standard deviation from averaging multiple measurements.

The identification of the corresponding organic compounds was limited by the high fragmentation due to the electron impact ionization operated in the HR-ToF-AMS instrument. Further identification was investigated conducted by LC-MS on with liquid AS solutions. In EXP C1 and C2, an aqueous solution of ammonium sulfate (99.5 %) at 1.5 M was directly 370 injected and was analyzed in the positive mode. The acetonitrile and methanol eluents showed similar results for compound separation. Figure 7 shows a chromatogram of this an ammonium sulfate solution (green line) as well as blanks of Milli-Q water (red line) and Fisher water (blue line). In Milli-Q water, two ions were present at retention times 4.45 min and 4.65 min, their mass spectra were attributed as nylon polymers (C₆H₁₁NO)_n which are among the frequently reported interfering compounds (Tran and Doucette, 2006; Keller et al., 2008)(Tran and Doucette, 2006; Keller et al., 2008). However, no

375 significant contamination was observed in the Fisher water (LC-MS Grade). Figure 7 shows that the same ions found in Milli-Q water were also present in the AS solution prepared in the same Milli-Q water. Many other ions were detected in the AS solution, and their retention times highly suggested that these molecules were organic. The proposed raw formulas systematically contained carbon, hydrogen, oxygen, nitrogen and sometimes sulfur, consistent with the HR-ToF-AMS spectra. The double bond equivalence (DBE) varies from 1.5 to 5.5 showing that the molecules are unsaturated and potentially cyclic.

380 Different to nylon polymers found in Milli-Q water, these raw formula are not referenced among the common laboratory LC-MS contaminants (Keller et al., 2008). The mass error was always well below 5 ppm and no raw formula with sodium adduct was suggested ~~that most intense ions detected in the AS solution are described in more details in SI6, where some. Some of the m/z showed two different retention times, implying potentially the presence of isomers, for. For example, at m/z 225.1600 and 226.1918, two peaks were detected, one at 2.89 minutes and the other at 3.11 minutes as described in detail in SI8 for the most intense ions. In the negative ESI mode, the signal was overwritten by the sulfate ion (detected at [M+H]⁻ : 96.9596, HSO₄⁻) along the whole chromatogram, due to the high ammonium sulfate concentrations used.~~

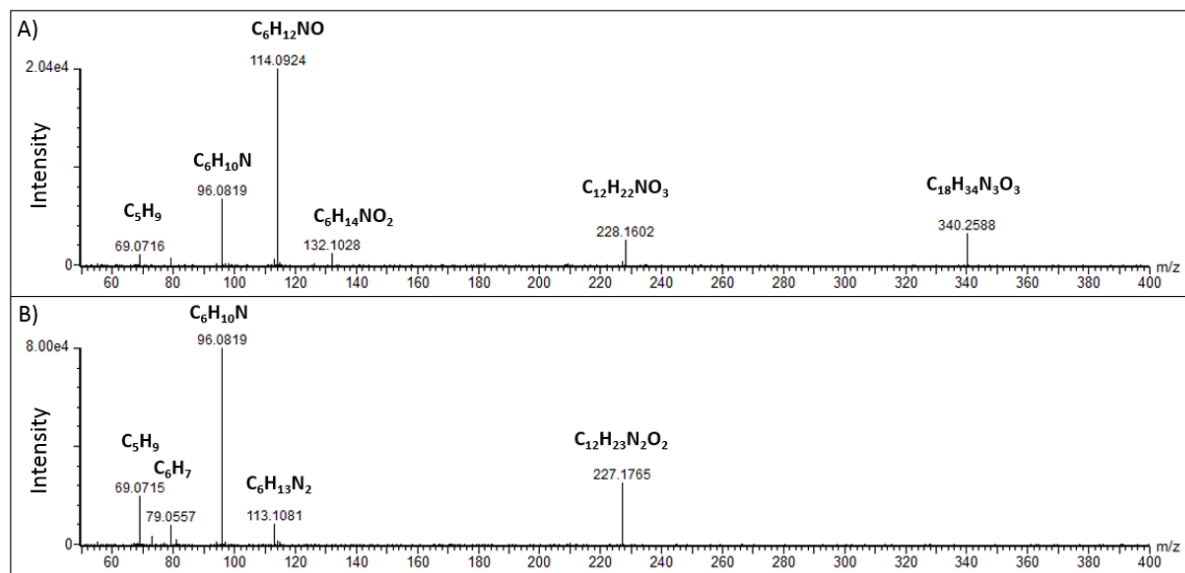
385



390 **Figure 7:** LC/ESI⁺-MS base peak chromatogram of Milli-Q water, Fisher water and AS (99.5 %) solution of 1.5 M (EXP C1) with corresponding major ion masses associated with raw formulas. The bold ion masses and proposed raw formula were studied in MS-MS (EXP C9). Ions marked with * were detected in their [M-H]⁻ form in LC/ESI-MS (in EXP C6-8).

For further identification and for detection in the negative mode, AS crystals and solutions at various concentrations were extracted using different solvents and different methods (C3-7 in Table 2). In the positive mode, more than 60 % of the molecules identified by direct injection without the extraction step were also detected. Compared to other solvents, acetonitrile

was found to be the most efficient extracting solvent. In the negative mode, the signal was systematically much lower (ion current intensity $< 10^3$ counts per second) and only molecules marked aswith* in Fig. 7 were detected. Consequently, no further analysis was performed in the negative mode due to the low signal. In EXP C8 and C10, another markbrand of AS crystals of the same purity (99.5 %) was tested for comparison, ~~and revealed that some. Some~~ common ions were detected ~~(in the extracts)~~ in the positive mode, but at a much lower intensity (by a factor of ~ 20 , see SI9), thus demonstrating that the detected organic compounds were present in both AS crystals and that the level of organic contamination depends at least in part on the AS markbrand. EMSURE® products are supposed to offer a high level of quality and appear to be less contaminated despite the same reported purity. Figure 8 shows the MS-MS measurements operated on two ions detected in EXP C9 (see SI7SI10 for the complete MS-MS results). These results support the proposed raw formula, confirming that these organic compounds contained oxygen and nitrogen and/or sulfur. They also show recurrent fragments: for instance, fragment ion at m/z 96.082, most likely described by the raw formula $C_6H_{10}N$, was found in all the MS-MS spectra as well as the fragment ion at m/z 69.072 corresponding to C_5H_9 which was also a fragment observed in the spectra from the HR-ToF-AMS. ~~However, the latter instrument did not detect fragments at $m/z > 100$ due to electron impact ionization that induce high fragmentation with high intensity.~~



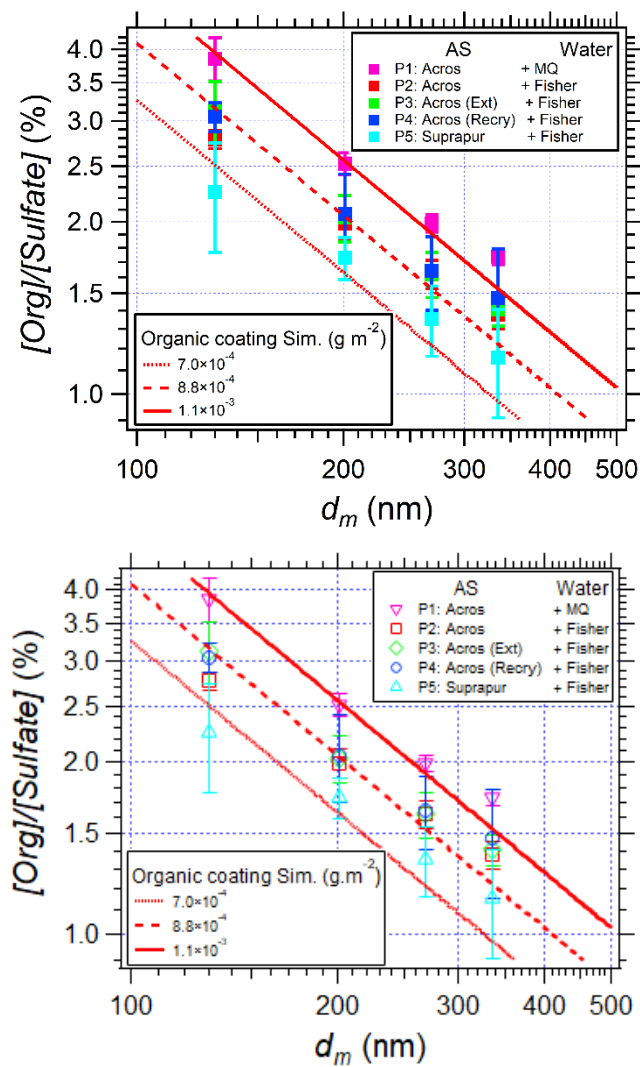
410 **Figure 8:** Mass spectra obtained from LC/ESI⁺-MS-MS measurements of two detected compounds in EXP C9. The $[M+H]^+$ ions were detected at : A) m/z 340, using a collision energy of 25 eV; and B) m/z 227, using a collision energy of 20 eV.

These results confirm that the organic compounds present in AS are large molecules: out of the 20 most intense detected molecules, 12 contained 12 carbon atoms (C_{12}), and the others contained C_6 (2 molecules bearing $C_xH_yN_{1/2}$), C_{10} (1 molecule), C_{11} (1 molecule), C_{17} (1 molecule), C_{18} (2 molecules) and up to C_{24} (1 molecule), with m/z ranging from 96 to 533.

Apart from the 2 smallest molecules (C_6), all of them bear mono- or poly-functional groups with at least 2 heteroatoms (N and O are always present, and S is found in 10 molecules) confirming their low volatility. Most of them fragment following the same scheme, thus showing similar structures. No structure is proposed here as there are many possible structures. The fact that these molecules were largely detected in the positive mode and that they all bear at least one N atom, and the fact that they were observed specifically at the surface of the ~~suspended~~-AS aerosol particles, could suggest that they are cationic surfactants such as quaternary ammonium salts remaining from the manufacturing processes. Ammonium sulfate is typically produced by the reaction of gaseous ammonia with sulfuric acid, but the precise manufacturing processes and raw materials of the suppliers are not known in detail and therefore do not allow us to draw any conclusions for these processes.

420 3.5 Removing organic traces from AS ~~suspended~~aerosol particles

425 To give recommendations on the use of AS for laboratory studies or instrument calibrations with organic contaminations as low as possible, the results of EXP P2 to P5 using high quality water and AS or purified AS crystals, are shown in Figure 9 where $[Org]/[Sulfate]$ is plotted versus particle size.



430 **Figure 9** : $[\text{Org}]/[\text{Sulfate}]$ in AS suspended aerosol particles as function of mobility diameter in EXP P1 to P5. The red lines represent the calculated $[\text{Org}]/[\text{Sulfate}]$ simulating surface coating of organic matter (from Eq. 3) for EXP P1, P4 and P5.

Figure 9 shows that, although decreasing with increasing purification, organic traces remain present in all experiments. They seem to remain coated at the surface of the particles, as shown by the good agreement between the 435 simulations and experimental data. According to the simulation results, a reduction of 20 % of $[\text{Org}]/[\text{Sulfate}]$ ratios is observed when Fisher water (red squares) replaces Milli-Q water (pink squares). This reduction might be due to the removing of Nylon polymers found in Milli-Q water (Figure 7). However, no significant difference is observed between EXP P2, P3 and P4, i.e., purification of AS crystals by acetonitrile or recrystallization are not sufficiently efficient to remove organic traces. Finally, comparing EXP P5 (cyan squares) and P2 (red squares), another 20 % reduction of organic traces is observed when

440 highly pure AS crystals were used (99.9999 %). In this case, the organic traces are lower than 2.5 % on the AS particles-with
 $d_m = 130$ to 336 nm (corresponding to $d_a = 200$ to 500 nm).

4. Conclusions and implications

445 Ammonium sulfate is one of the dominant components of atmospheric aerosol and is widely used in laboratory experiments and for instrument calibration purposes. However, the widely used commercial AS crystals may contain interfering organic impurities. To answer questions related to the quantity and the quality of organic impurities found in a wide range of widely used commercial AS products, a series of experiments were performed to quantify and identify organic impurities on AS suspended aerosol particles and in liquid solutions using a HR-ToF-AMS and a LC-MS. The results showed that, using 99.5 % purity AS, up to 3.8 % of organic impurities were present related to sulfate mass. This ratio was found to be independent of the concentration of nebulized AS solutions but was inversely related to the particle size. The simulations 450 of AS-Organic mixtures showed a homogeneous organic coating on the surface of AS particles with a constant surface density of 1.4×10^{-3} g.m⁻². Regarding to the particle size selection system, the comparison between AAC and DMA showed consistent [Org]/[Sulfate] ratio mass ratios, thus highlighting that the observed particle size effects were not due to instrumental artifacts. The chemical Using LC-MS analysis of the organic content showed that their structures are independent to the particle size. Up up to 20 different stable highly functionalized molecules have been detected in AS 455 solutions with nitrate, amin, and consistent or sulphate groups. The proposed raw formulas were proposed. Theses formulas include included mostly C₁₂ compounds with mono- or poly-functional groups with at least two heteroatoms (N and O were always present, and S was found in 10 molecules) confirming their suggesting low volatility. As these These nitrogenous molecules were largely abundantly detected by LC-MS in AS solutions in the positive ESI mode by LC MS, all carrying at least one nitrogen atom. Based on the observation that, and in the nebulized solutions, they are were observed to be coated 460 at on the surface of the suspended AS aerosol particles. It can Thus, it could be suggested that they are might comprise cationic surfactants such as quaternary ammonium salts remaining from the manufacturing processes.

465 The presence of low volatile, probably surface active organic compounds in commercial AS products is extremely important for laboratory aerosol studies. From this suggestion, the potential effects of organic impurities on CCN activation of AS aerosols were investigated, to determine the error made on the critical supersaturation if one assumes 100% AS, omitting the presence of organic impurities. This estimation was performed with a simple calculation using the κ -Köhler equation (Petters and Kreidenweis, 2007), see SI11 for details. For the estimation of the critical supersaturation in the presence of organic impurities, two extreme hypotheses were explored. In hypothesis 1, the organic fraction was considered soluble and non-surface-active, whereas in hypothesis 2, it was considered extremely surface-active, using the most powerful surfactant as a proxy. Following each of these hypotheses, the supersaturation was calculated along the droplet activation of an AS particle of 130 nm with and without organic impurities (Fig. SI11). The results show that whereas the critical supersaturation of AS

aerosols is not significantly impacted by the presence of organic impurities under hypothesis 1, it is highly impacted under hypothesis 2, with a potential error of more than 70%.

475 In view of these extreme results, and especially the very important error observed for surface-active compounds, the potential quantity of surface-active species contained in AS solutions (Across 99.5 % diluted in Milli-Q water) was investigated (SI12). The results showed that AS solutions contain extremely low amounts of cationic and non-ionic surfactants and an upper limit of [Org surfactant]/[Sulfate] mass ratio of 1×10^{-5} % was determined. Although this ratio is five orders of magnitude lower than the total organic fraction detected in AS particles, the potential effect of these surfactants on the surface tension of 130 nm diameter AS particles was investigated. For such particles, the obtained [Org surfactant]/[Sulfate] mass ratio induces a concentration of 6×10^{-7} mol.L⁻¹ of surfactants. At this very low concentration, even the most surface-active molecules show a surface tension similar to that of pure water as shown by surface tension isotherms (Ekström et al., 2010; Frossard et al., 2019; Arabadzhieva et al., 2020). It was thus concluded that the CCN activity of AS particles with $d_m = 130$ nm should not be significantly affected by the presence of the organic impurities. However, caution should be taken to keep their amounts as low as possible.

480 In this work, some efforts to remove these organic impurities have been tentatively tested by purifying and recrystallizing AS crystals. Though no significant difference was observed, it is likely that better results could be obtained by increasing the number of purification and recrystallization cycles, as very high purity AS crystals (99.9999 %) showed significantly lower organic content. It is therefore recommended to use AS seeds with caution, especially when small particles are used, in terms of AS purity and water purity when aqueous solutions are used for atomization.

Appendix A: Morphological properties of AS aerosols

490 Following the method of Zelenyuk et al., (2006), the shape factor (χ) in any flow regime (continuous and transient) can be determined by the ratio of d_{va}/d_m in Eq. A1.

$$\frac{d_{va}}{d_m} = \frac{\rho_p}{\rho_0} \frac{1}{\chi^2} \frac{C_c(d_{va}\chi \rho_p/\rho_0)}{C_c(d_m)} \quad (A1)$$

Where ρ_p is the particle density, ρ_0 is the standard density noticed as 1 g.cm⁻³, C_c is the Cunningham slip factor (Kim et al., 2005) Where ρ_p is the particle density, ρ_0 is the standard density noticed as 1 g.cm⁻³, C_c is the Cunningham slip factor (Kim et al., 2005), given by Eq. A2.

$$C_c(K_n) = 1 + K_n \left[1.165 + 0.483 \exp \left(-\frac{0.997}{K_n} \right) \right] \quad (A2)$$

495 $K_n(d) = 2\lambda_g/d$ is the Knudsen number, and λ_g is the gas mean free path. In this work, normal temperature and pressure (293.15 K at 1 atm) were applied for the calculation of the shape factor of AS aerosols.

The shape factor (χ) of monodisperse AS aerosols selected by the AAC was calculated according to Eq. A1 and is shown in Table A1, together with the aerodynamic diameter (d_a) selected in the AAC, the mobility diameter d_m and the vacuum aerodynamic diameter d_{va} representing the average mode of size distributions given by the SMPS and HR-ToF-AMS (p-ToF

500 mode), respectively. Table A1 shows that, within the uncertainty, the selected AS particles own a size-independent shape factor of 1.06, which falls in the interval of 1.03 and 1.07 reported by (Zelenyuk et al., 2006).

Table A1: Morphological properties of monodisperse AS aerosols selected by the AAC (in EXP P1 and P2): aerodynamic diameter (d_a), mobility diameter (d_m), vacuum aerodynamic diameter (d_{va}), and shape factor (χ). The uncertainty represents the standard deviation of several measurements under the same selection condition.

d_a (nm)	d_m (nm)	d_{va} (nm)	Shape factor (χ)
200	126.6 ± 0.3	206 ± 6	1.05 ± 0.02
300	194.3 ± 0.3	312 ± 8	1.06 ± 0.02
400	267.6 ± 0.4	429 ± 10	1.06 ± 0.02
500	340.3 ± 0.4	539 ± 11	1.07 ± 0.02

505

Author contribution:

JW and AM provided the initial idea of this work. JW and ~~BFBTR~~ performed the experiments and data analysis of AS aerosol characterization with the HR-ToF-AMS. NB and SR carried out the measurements of AS solutions with the LC-MS. JW, NB and ~~JGJLC~~ proposed different purification processes of AS aerosols. The organic-inorganic mixing model was provided firstly by JW and improved by ~~BRBTR~~ and AM. JW, NB, ~~JGJMGS~~ and AM developed the structure of this paper. JW summarized all contributions and expressed them in this paper. All authors provided advice regarding ~~to the improvement~~improvements of this paper as well as to the writing of the final version of the manuscript.

Acknowledgements:

The authors acknowledge the support from the French National Research Agency (ANR-PRCI) ~~and the German Research Foundation (DFG)~~ through the ~~project~~projects PARAMOUNT (ANR18-CE92-0038-02). ~~The authors also thank the support from the project)~~ and ORACLE (ANR-20-CE93-0008-01_ACT) ~~from ANR-PRCI~~, as well as the French CNRS-LEFE-CHAT (Programme National-Les Enveloppes Fluides et l'Environnement-Chimie Atmosphérique – Project “SURFACTS”). The authors would like to thank two colleagues, Jim GRISILLON and Fabien ROBERT-PEILLARD, from the laboratory LCE - Aix Marseille University, who performed additional measurements for the quantification of surfactants in an AS solution. Finally, the authors acknowledge the 1st anonymous reviewer for her/his extremely thorough comments on the manuscript!

References

Abbatt, J. P. D., Broekhuizen, K., and Pradeep Kumar, P.: Cloud condensation nucleus activity of internally mixed ammonium sulfate/organic acid aerosol particles, *Atmos. Environ.*, 39, 4767–4778, <https://doi.org/10.1016/j.atmosenv.2005.04.029>, 2005.

Aiken, A. C., DeCarlo, P. F., and Jimenez, J. L.: Elemental Analysis of Organic Species with Electron Ionization High-
525 Resolution Mass Spectrometry, *Anal. Chem.*, 79, 8350–8358, <https://doi.org/10.1021/ac071150w>, 2007.

Andreae, M. O. and Rosenfeld, D.: Aerosol–cloud–precipitation interactions. Part 1. The nature and sources of cloud-active aerosols, *Earth-Sci. Rev.*, 89, 13–41, <https://doi.org/10.1016/j.earscirev.2008.03.001>, 2008.

[Arabadzhieva, D., Tchoukov, P., and Mileva, E.: Impact of Adsorption Layer Properties on Drainage Behavior of Microscopic Foam Films: The Case of Cationic/Nonionic Surfactant Mixtures, *Colloids Interfaces*, 4, 53, 530 <https://doi.org/10.3390/colloids4040053>, 2020.](#)

Badger, C. L., George, I., Griffiths, P. T., Braban, C. F., Cox, R. A., and Abbatt, J. P. D.: Phase transitions and hygroscopic growth of aerosol particles containing humic acid and mixtures of humic acid and ammonium sulphate, *Atmospheric Chem. Phys.*, 6, 755–768, <https://doi.org/10.5194/acp-6-755-2006>, 2006.

Brooks, S. D., DeMott, P. J., and Kreidenweis, S. M.: Water uptake by particles containing humic materials and mixtures of humic materials with ammonium sulfate, *Atmos. Environ.*, 38, 1859–1868, <https://doi.org/10.1016/j.atmosenv.2004.01.009>, 2004.

[Brüggemann, M., Xu, R., Tilgner, A., Kwong, K. C., Mutzel, A., Poon, H. Y., Otto, T., Schaefer, T., Poulain, L., Chan, M. N., and Herrmann, H.: Organosulfates in Ambient Aerosol: State of Knowledge and Future Research Directions on Formation, Abundance, Fate, and Importance, *Environ. Sci. Technol.*, 54, 3767–3782, <https://doi.org/10.1021/acs.est.9b06751>, 2020.](#)

540 Canagaratna, M. R., Jimenez, J. L., Kroll, J. H., Chen, Q., Kessler, S. H., Massoli, P., Hildebrandt Ruiz, L., Fortner, E., Williams, L. R., Wilson, K. R., Surratt, J. D., Donahue, N. M., Jayne, J. T., and Worsnop, D. R.: Elemental ratio measurements of organic compounds using aerosol mass spectrometry: characterization, improved calibration, and implications, *Atmospheric Chem. Phys.*, 15, 253–272, <https://doi.org/10.5194/acp-15-253-2015>, 2015.

Charlson, R. J., Schwartz, S., Hales, J., Cess, R. D., Coakley, J. J., Hansen, J., and Hofmann, D.: Climate forcing by 545 anthropogenic aerosols, *Science*, 255, 423–430, 1992.

Clegg, S. L., Brimblecombe, P., and Wexler, A. S.: Thermodynamic Model of the System $\text{H}^+ + \text{NH}_4^+ + \text{Na}^+ + \text{SO}_4^{2-} + \text{NO}_3^- + \text{Cl}^- - \text{H}_2\text{O}$ at 298.15 K, *J. Phys. Chem. A*, 102, 2155–2171, <https://doi.org/10.1021/jp973043j>, 1998.

Darer, A. I., Cole-Filipliak, N. C., O'Connor, A. E., and Elrod, M. J.: Formation and stability of atmospherically relevant isoprene-derived organosulfates and organonitrates, *Environ. Sci. Technol.*, 45, 1895–1902, 2011.

550 De Haan, D. O., Hawkins, L. N., Welsh, H. G., Pednekar, R., Casar, J. R., Pennington, E. A., de Loera, A., Jimenez, N. G., Symons, M. A., Zauscher, M., Pajunoja, A., Caponi, L., Cazaunau, M., Formenti, P., Gratien, A., Pangui, E., and Doussin, J.-F.: Brown Carbon Production in Ammonium- or Amine-Containing Aerosol Particles by Reactive Uptake of Methylglyoxal and Photolytic Cloud Cycling, *Environ. Sci. Technol.*, 51, 7458–7466, <https://doi.org/10.1021/acs.est.7b00159>, 2017.

DeCarlo, P. F., Slowik, J. G., Worsnop, D. R., Davidovits, P., and Jimenez, J. L.: Particle Morphology and Density 555 Characterization by Combined Mobility and Aerodynamic Diameter Measurements. Part 1: Theory, *Aerosol Sci. Technol.*, 38, 1185–1205, <https://doi.org/10.1080/027868290903907>, 2004.

DeCarlo, P. F., Kimmel, J. R., Trimborn, A., Northway, M. J., Jayne, J. T., Aiken, A. C., Gonin, M., Fuhrer, K., Horvath, T., Docherty, K. S., Worsnop, D. R., and Jimenez, J. L.: Field-Deployable, High-Resolution, Time-of-Flight Aerosol Mass Spectrometer, *Anal. Chem.*, 78, 8281–8289, <https://doi.org/10.1021/ac061249n>, 2006.

560 Ekström, S., Nozière, B., Hultberg, M., Alsberg, T., Magnér, J., Nilsson, E. D., and Artaxo, P.: A possible role of ground-based microorganisms on cloud formation in the atmosphere, *Biogeosciences*, 7, 387–394, <https://doi.org/10.5194/bg-7-387-2010, 2010>.

Engelhart, G. J., Asa-Awuku, A., Nenes, A., and Pandis, S. N.: CCN activity and droplet growth kinetics of fresh and aged monoterpane secondary organic aerosol, *Atmospheric Chem. Phys.*, 8, 3937–3949, <https://doi.org/10.5194/acp-8-3937-2008, 2008>.

565 Frossard, A. A., Gérard, V., Duplessis, P., Kinsey, J. D., Lu, X., Zhu, Y., Bisgrove, J., Maben, J. R., Long, M. S., Chang, R. Y.-W., Beaupré, S. R., Kieber, D. J., Keene, W. C., Nozière, B., and Cohen, R. C.: Properties of Seawater Surfactants Associated with Primary Marine Aerosol Particles Produced by Bursting Bubbles at a Model Air–Sea Interface, *Environ. Sci. Technol.*, 53, 9407–9417, <https://doi.org/10.1021/acs.est.9b02637, 2019>.

570 Gérard, V., Nozière, B., Fine, L., Ferronato, C., Singh, D. K., Frossard, A. A., Cohen, R. C., Asmi, E., Lihavainen, H., Kivekäs, N., Aurela, M., Brus, D., Frka, S., and Cvitešić Kušan, A.: Concentrations and Adsorption Isotherms for Amphiphilic Surfactants in PM1 Aerosols from Different Regions of Europe, *Environ. Sci. Technol.*, 53, 12379–12388, <https://doi.org/10.1021/acs.est.9b03386, 2019>.

Grace, D. N., Lugos, E. N., Ma, S., Griffith, D. R., Hendrickson, H. P., Woo, J. L., and Galloway, M. M.: Brown Carbon 575 Formation Potential of the Biacetyl–Ammonium Sulfate Reaction System, *ACS Earth Space Chem.*, 4, 1104–1113, <https://doi.org/10.1021/acsearthspacechem.0c00096, 2020>.

Hämeri, K., Charlson, R., and Hansson, H.-C.: Hygroscopic properties of mixed ammonium sulfate and carboxylic acids particles, *AIChE J.*, 48, 1309–1316, <https://doi.org/10.1002/aic.690480617, 2002>.

580 Hawkins, L. N., Welsh, H. G., and Alexander, M. V.: Evidence for pyrazine-based chromophores in cloud water mimics containing methylglyoxal and ammonium sulfate, *Atmospheric Chem. Phys.*, 18, 12413–12431, <https://doi.org/10.5194/acp-18-12413-2018, 2018>.

Hensley, J. C., Birdsall, A. W., Valtierra, G., Cox, J. L., and Keutsch, F. N.: Revisiting the reaction of dicarbonyls in aerosol proxy solutions containing ammonia: the case of butenedial, *Atmospheric Chem. Phys.*, 21, 8809–8821, <https://doi.org/10.5194/acp-21-8809-2021, 2021>.

585 Herrmann, H.: Kinetics of Aqueous Phase Reactions Relevant for Atmospheric Chemistry, *Chem. Rev.*, 103, 4691–4716, <https://doi.org/10.1021/cr020658q, 2003>.

Hu, K. S., Darer, A. I., and Elrod, M. J.: Thermodynamics and kinetics of the hydrolysis of atmospherically relevant organonitrates and organosulfates, *Atmospheric Chem. Phys.*, 11, 8307–8320, <https://doi.org/10.5194/acp-11-8307-2011, 2011>.

590 [Inuma, Y., Müller, C., Berndt, T., Böge, O., Claeys, M., and Herrmann, H.: Evidence for the Existence of Organosulfates from \$\beta\$ -Pinene Ozonolysis in Ambient Secondary Organic Aerosol, Environ. Sci. Technol., 41, 6678–6683, <https://doi.org/10.1021/es070938t>, 2007.](https://doi.org/10.1021/es070938t)

IPCC: Climate Change 2013 – The Physical Science Basis: Working Group I Contribution to the Fifth Assessment Report of the Intergovernmental Panel on Climate Change, Cambridge University Press, Cambridge, 595 <https://doi.org/10.1017/CBO9781107415324>, 2013.

Jimenez, J. L., Canagaratna, M. R., Donahue, N. M., Prevot, A. S. H., Zhang, Q., Kroll, J. H., DeCarlo, P. F., Allan, J. D., Coe, H., Ng, N. L., Aiken, A. C., Docherty, K. S., Ulbrich, I. M., Grieshop, A. P., Robinson, A. L., Duplissy, J., Smith, J. D., Wilson, K. R., Lanz, V. A., Hueglin, C., Sun, Y. L., Tian, J., Laaksonen, A., Raatikainen, T., Rautiainen, J., Vaattovaara, P., Ehn, M., Kulmala, M., Tomlinson, J. M., Collins, D. R., Cubison, M. J., E, Dunlea, J., Huffman, J. A., Onasch, T. B., Alfarra, M. R., 600 Williams, P. I., Bower, K., Kondo, Y., Schneider, J., Drewnick, F., Borrmann, S., Weimer, S., Demerjian, K., Salcedo, D., Cottrell, L., Griffin, R., Takami, A., Miyoshi, T., Hatakeyama, S., Shimono, A., Sun, J. Y., Zhang, Y. M., Dzepina, K., Kimmel, J. R., Sueper, D., Jayne, J. T., Herndon, S. C., Trimborn, A. M., Williams, L. R., Wood, E. C., Middlebrook, A. M., Kolb, C. E., Baltensperger, U., and Worsnop, D. R.: Evolution of Organic Aerosols in the Atmosphere, *Science*, 326, 1525–1529, <https://doi.org/10.1126/science.1180353>, 2009.

605 [Jimenez, N. G., Sharp, K. D., Gramyk, T., Ugland, D. Z., Tran, M.-K., Rojas, A., Rafla, M. A., Stewart, D., Galloway, M. M., Lin, P., Laskin, A., Cazaunau, M., Pangui, E., Doussin, J.-F., and De Haan, D. O.: Radical-Initiated Brown Carbon Formation in Sunlit Carbonyl–Amine–Ammonium Sulfate Mixtures and Aqueous Aerosol Particles, *ACS Earth Space Chem.*, 6, 228–238, <https://doi.org/10.1021/acsearthspacechem.1c00395>, 2022.](https://doi.org/10.1021/acsearthspacechem.1c00395)

Johnson, T. J., Irwin, M., Symonds, J. P. R., Olfert, J. S., and Boies, A. M.: Measuring aerosol size distributions with the 610 aerodynamic aerosol classifier, *Aerosol Sci. Technol.*, 52, 655–665, <https://doi.org/10.1080/02786826.2018.1440063>, 2018.

Kampf, C. J., Jakob, R., and Hoffmann, T.: Identification and characterization of aging products in the glyoxal/ammonium sulfate system – implications for light-absorbing material in atmospheric aerosols, *Atmospheric Chem. Phys.*, 12, 6323–6333, <https://doi.org/10.5194/acp-12-6323-2012>, 2012.

Keller, B. O., Sui, J., Young, A. B., and Whittal, R. M.: Interferences and contaminants encountered in modern mass 615 spectrometry, *Anal. Chim. Acta*, 627, 71–81, <https://doi.org/10.1016/j.aca.2008.04.043>, 2008.

[Kiendler-Scharr, A., Mensah, A. A., Fries, E., Topping, D., Nemitz, E., Prevot, A. S. H., Äijälä, M., Allan, J., Canonaco, F., Canagaratna, M., Carbone, S., Crippa, M., Dall Osto, M., Day, D. A., De Carlo, P., Di Marco, C. F., Elbern, H., Eriksson, A., Freney, E., Hao, L., Herrmann, H., Hildebrandt, L., Hillamo, R., Jimenez, J. L., Laaksonen, A., McFiggans, G., Mohr, C., O'Dowd, C., Otjes, R., Ovadnevaite, J., Pandis, S. N., Poulain, L., Schlag, P., Sellegrini, K., Swietlicki, E., Tiitta, P., Vermeulen, A., Wahner, A., Worsnop, D., and Wu, H.-C.: Ubiquity of organic nitrates from nighttime chemistry in the European submicron aerosol, *Geophys. Res. Lett.*, 43, 7735–7744, <https://doi.org/10.1002/2016GL069239>, 2016.](https://doi.org/10.1002/2016GL069239)

Kim, J. H., Mulholland, G. W., Kukuck, S. R., and Pui, D. Y. H.: Slip Correction Measurements of Certified PSL Nanoparticles Using a Nanometer Differential Mobility Analyzer (Nano-DMA) for Knudsen Number From 0.5 to 83, *J. Res. Natl. Inst. Stand. Technol.*, 110, 31–54, <https://doi.org/10.6028/jres.110.005>, 2005.

625 Kind, T. and Fiehn, O.: Seven Golden Rules for heuristic filtering of molecular formulas obtained by accurate mass spectrometry, *BMC Bioinformatics*, 8, 105, <https://doi.org/10.1186/1471-2105-8-105>, 2007.

King, S. M., Rosenoern, T., Shilling, J. E., Chen, Q., and Martin, S. T.: Increased cloud activation potential of secondary organic aerosol for atmospheric mass loadings, *Atmospheric Chem. Phys.*, 9, 2959–2971, <https://doi.org/10.5194/acp-9-2959-2009>, 2009.

630 Koehler, K. A., Kreidenweis, S. M., DeMott, P. J., Prenni, A. J., Carrico, C. M., Ervens, B., and Feingold, G.: Water activity and activation diameters from hygroscopicity data - Part II: Application to organic species, *Atmospheric Chem. Phys.*, 6, 795–809, <https://doi.org/10.5194/acp-6-795-2006>, 2006.

Laskin, J., Laskin, A., Nizkorodov, S. A., Roach, P., Eckert, P., Gilles, M. K., Wang, B., Lee, H. J. (Julie), and Hu, Q.: Molecular Selectivity of Brown Carbon Chromophores, *Environ. Sci. Technol.*, 48, 12047–12055, <https://doi.org/10.1021/es503432r>, 2014.

635 Liggio, J., Li, S. M., and McLaren, R.: Heterogeneous Reactions of Glyoxal on Particulate Matter: Identification of Acetals and Sulfate Esters, *Environ. Sci. Technol.*, 39, 1532–1541, <https://doi.org/10.1021/es048375y>, 2005.

Meyer, N. K., Duplissy, J., Gysel, M., Metzger, A., Dommen, J., Weingartner, E., Alfarra, M. R., Prevot, A. S. H., Fletcher, C., Good, N., McFiggans, G., Jonsson, Å. M., Hallquist, M., Baltensperger, U., and Ristovski, Z. D.: Analysis of the 640 hygroscopic and volatile properties of ammonium sulphate seeded and unseeded SOA particles, *Atmospheric Chem. Phys.*, 9, 721–732, <https://doi.org/10.5194/acp-9-721-2009>, 2009.

Moore, R. H., Ingall, E. D., Sorooshian, A., and Nenes, A.: Molar mass, surface tension, and droplet growth kinetics of marine organics from measurements of CCN activity, *Geophys. Res. Lett.*, 35, <https://doi.org/10.1029/2008GL033350>, 2008.

Nandy, L. and Dutcher, C. S.: Phase Behavior of Ammonium Sulfate with Organic Acid Solutions in Aqueous Aerosol Mimics 645 Using Microfluidic Traps, *J. Phys. Chem. B*, 122, 3480–3490, <https://doi.org/10.1021/acs.jpcb.7b10655>, 2018.

Nozière, B., Dziedzic, P., and Córdova, A.: Inorganic ammonium salts and carbonate salts are efficient catalysts for aldol condensation in atmospheric aerosols, *Phys. Chem. Chem. Phys.*, 12, 3864–3872, <https://doi.org/10.1039/B924443C>, 2010.

650 Nozière, B., Baduel, C., and Jaffrezo, J.-L.: The dynamic surface tension of atmospheric aerosol surfactants reveals new aspects of cloud activation, *Nat. Commun.*, 5, 3335, <https://doi.org/10.1038/ncomms4335>, 2014.

Ovadnevaite, J., Zuend, A., Laaksonen, A., Sanchez, K. J., Roberts, G., Ceburnis, D., Decesari, S., Rinaldi, M., Hodas, N., Facchini, M. C., Seinfeld, J. H., and O' Dowd, C.: Surface tension prevails over solute effect in organic-influenced cloud droplet activation, *Nature*, 546, 637–641, <https://doi.org/10.1038/nature22806>, 2017.

Petters, M. D.: A language to simplify computation of differential mobility analyzer response functions, *Aerosol Sci. Technol.*, 52, 1437–1451, <https://doi.org/10.1080/02786826.2018.1530724>, 2018.

655 Petters, M. D. and Kreidenweis, S. M.: A single parameter representation of hygroscopic growth and cloud condensation nucleus activity, *Atmospheric Chem. Phys.*, 7, 1961–1971, <https://doi.org/10.5194/acp-7-1961-2007>, 2007.

Petters, M. D. and Kreidenweis, S. M.: A single parameter representation of hygroscopic growth and cloud condensation nucleus activity – Part 3: Including surfactant partitioning, *Atmospheric Chem. Phys.*, 13, 1081–1091, <https://doi.org/10.5194/acp-13-1081-2013>, 2013.

660 Pieber, S. M., El Haddad, I., Slowik, J. G., Canagaratna, M. R., Jayne, J. T., Platt, S. M., Bozzetti, C., Daellenbach, K. R., Fröhlich, R., Vlachou, A., Klein, F., Dommen, J., Miljevic, B., Jiménez, J. L., Worsnop, D. R., Baltensperger, U., and Prévôt, A. S. H.: Inorganic Salt Interference on CO₂ in Aerodyne AMS and ACSM Organic Aerosol Composition Studies, *Environ. Sci. Technol.*, 50, 10494–10503, <https://doi.org/10.1021/acs.est.6b01035>, 2016.

Pöschl, U. and Shiraiwa, M.: Multiphase Chemistry at the Atmosphere–Biosphere Interface Influencing Climate and Public Health in the Anthropocene, *Chem. Rev.*, 115, 4440–4475, <https://doi.org/10.1021/cr500487s>, 2015.

665 Powelson, M. H., Espelien, B. M., Hawkins, L. N., Galloway, M. M., and De Haan, D. O.: Brown Carbon Formation by Aqueous-Phase Carbonyl Compound Reactions with Amines and Ammonium Sulfate, *Environ. Sci. Technol.*, 48, 985–993, <https://doi.org/10.1021/es4038325>, 2014.

Prenni, A. J., DeMott, P. J., and Kreidenweis, S. M.: Water uptake of internally mixed particles containing ammonium sulfate and dicarboxylic acids, *Atmos. Environ.*, 37, 4243–4251, [https://doi.org/10.1016/S1352-2310\(03\)00559-4](https://doi.org/10.1016/S1352-2310(03)00559-4), 2003.

670 Prisle, N. L.: A predictive thermodynamic framework of cloud droplet activation for chemically unresolved aerosol mixtures, including surface tension, non-ideality, and bulk–surface partitioning, *Atmospheric Chem. Phys.*, 21, 16387–16411, <https://doi.org/10.5194/acp-21-16387-2021>, 2021.

Saukko, E., Zorn, S., Kuwata, M., Keskinen, J., and Virtanen, A.: Phase State and Deliquescence Hysteresis of Ammonium-Sulfate-Seeded Secondary Organic Aerosol, *Aerosol Sci. Technol.*, 49, 531–537, <https://doi.org/10.1080/02786826.2015.1050085>, 2015.

675 Seinfeld, J. H., Bretherton, C., Carslaw, K. S., Coe, H., DeMott, P. J., Dunlea, E. J., Feingold, G., Ghan, S., Guenther, A. B., Kahn, R., Kraucunas, I., Kreidenweis, S. M., Molina, M. J., Nenes, A., Penner, J. E., Prather, K. A., Ramanathan, V., Ramaswamy, V., Rasch, P. J., Ravishankara, A. R., Rosenfeld, D., Stephens, G., and Wood, R.: Improving our fundamental understanding of the role of aerosol–cloud interactions in the climate system, *Proc. Natl. Acad. Sci.*, 113, 5781–5790, <https://doi.org/10.1073/pnas.1514043113>, 2016.

680 Shakya, K. M. and Peltier, R. E.: Non-sulfate sulfur in fine aerosols across the United States: Insight for organosulfate prevalence, *Atmos. Environ.*, 100, 159–166, <https://doi.org/10.1016/j.atmosenv.2014.10.058>, 2015.

Sjogren, S., Gysel, M., Weingartner, E., Baltensperger, U., Cubison, M. J., Coe, H., Zardini, A. A., Marcolli, C., Krieger, U. K., and Peter, T.: Hygroscopic growth and water uptake kinetics of two-phase aerosol particles consisting of ammonium sulfate, adipic and humic acid mixtures, *J. Aerosol Sci.*, 38, 157–171, <https://doi.org/10.1016/j.jaerosci.2006.11.005>, 2007.

Smith, M. L., You, Y., Kuwata, M., Bertram, A. K., and Martin, S. T.: Phase Transitions and Phase Miscibility of Mixed Particles of Ammonium Sulfate, Toluene-Derived Secondary Organic Material, and Water, *J. Phys. Chem. A*, 117, 8895–8906, <https://doi.org/10.1021/jp405095e>, 2013.

690 Sorjamaa, R., Svenningsson, B., Raatikainen, T., Henning, S., Bilde, M., and Laaksonen, A.: The role of surfactants in Köhler theory reconsidered, *Atmospheric Chem. Phys.*, 4, 2107–2117, <https://doi.org/10.5194/acp-4-2107-2004>, 2004.

Stokes, R. H. and Robinson, R. A.: Interactions in Aqueous Nonelectrolyte Solutions. I. Solute-Solvent Equilibria, *J. Phys. Chem.*, 70, 2126–2131, <https://doi.org/10.1021/j100879a010>, 1966.

Surratt, J. D., Gómez-González, Y., Chan, A. W. H., Vermeylen, R., Shahgholi, M., Kleindienst, T. E., Edney, E. O., 695 Offenberg, J. H., Lewandowski, M., Jaoui, M., Maenhaut, W., Claeys, M., Flagan, R. C., and Seinfeld, J. H.: Organosulfate Formation in Biogenic Secondary Organic Aerosol, *J. Phys. Chem. A*, 112, 8345–8378, <https://doi.org/10.1021/jp802310p>, 2008.

Szmigielski, R.: Evidence for C5 organosulfur secondary organic aerosol components from in-cloud processing of isoprene: Role of reactive SO₄ and SO₃ radicals, *Atmos. Environ.*, 130, 14–22, <https://doi.org/10.1016/j.atmosenv.2015.10.072>, 2016.

700 Tavakoli, F. and Olfert, J. S.: An Instrument for the Classification of Aerosols by Particle Relaxation Time: Theoretical Models of the Aerodynamic Aerosol Classifier, *Aerosol Sci. Technol.*, 47, 916–926, <https://doi.org/10.1080/02786826.2013.802761>, 2013.

Tervahattu, H., Hartonen, K., Kerminen, V.-M., Kupiainen, K., Aarnio, P., Koskentalo, T., Tuck, A. F., and Vaida, V.: New evidence of an organic layer on marine aerosols, *J. Geophys. Res. Atmospheres*, 107, AAC 1-1-AAC 1-8, 705 <https://doi.org/10.1029/2000JD000282>, 2002.

Trainic, M., Abo Riziq, A., Lavi, A., Flores, J. M., and Rudich, Y.: The optical, physical and chemical properties of the products of glyoxal uptake on ammonium sulfate seed aerosols, *Atmospheric Chem. Phys.*, 11, 9697–9707, <https://doi.org/10.5194/acp-11-9697-2011>, 2011.

710 Tran, J. C. and Doucette, A. A.: Cyclic polyamide oligomers extracted from nylon 66 membrane filter disks as a source of contamination in liquid chromatography/mass spectrometry, *J. Am. Soc. Mass Spectrom.*, 17, 652–656, <https://doi.org/10.1016/j.jasms.2006.01.008>, 2006.

Treuel, L., Pederzani, S., and Zellner, R.: Deliquescence behaviour and crystallisation of ternary ammonium sulfate/dicarboxylic acid/water aerosols, *Phys. Chem. Chem. Phys.*, 11, 7976–7984, <https://doi.org/10.1039/B905007H>, 2009.

715 Varutbangkul, V., Brechtel, F. J., Bahreini, R., Ng, N. L., Keywood, M. D., Kroll, J. H., Flagan, R. C., Seinfeld, J. H., Lee, A., and Goldstein, A. H.: Hygroscopicity of secondary organic aerosols formed by oxidation of cycloalkenes, monoterpenes, sesquiterpenes, and related compounds, *Atmospheric Chem. Phys.*, 6, 2367–2388, <https://doi.org/10.5194/acp-6-2367-2006>, 2006.

Vepsäläinen, S., Calderón, S. M., Malila, J., and Prisle, N. L.: Comparison of six approaches to predicting droplet activation of surface active aerosol – Part 1: moderately surface active organics, *Atmospheric Chem. Phys.*, 22, 2669–2687, 720 <https://doi.org/10.5194/acp-22-2669-2022>, 2022.

Wach, P., Spólnik, G., Rudziński, K. J., Skotak, K., Claeys, M., Danikiewicz, W., and Szmigielski, R.: Radical oxidation of methyl vinyl ketone and methacrolein in aqueous droplets: Characterization of organosulfates and atmospheric implications, Chemosphere, 214, 1–9, <https://doi.org/10.1016/j.chemosphere.2018.09.026>, 2019.

Wex, H., Petters, M. D., Carrico, C. M., Hallbauer, E., Massling, A., McMeeking, G. R., Poulain, L., Wu, Z., Kreidenweis, S.

725 M., and Stratmann, F.: Towards closing the gap between hygroscopic growth and activation for secondary organic aerosol: Part 1 – Evidence from measurements, *Atmospheric Chem. Phys.*, 9, 3987–3997, <https://doi.org/10.5194/acp-9-3987-2009>, 2009.

Wiedensohler, A., Birmili, W., Nowak, A., Sonntag, A., Weinhold, K., Merkel, M., Wehner, B., Tuch, T., Pfeifer, S., Fiebig, M., Fjäraa, A. M., Asmi, E., Sellegrí, K., Depuy, R., Venzac, H., Villani, P., Laj, P., Aalto, P., Ogren, J. A., Swietlicki, E.,

730 Williams, P., Roldin, P., Quincey, P., Hüglin, C., Fierz-Schmidhauser, R., Gysel, M., Weingartner, E., Riccobono, F., Santos, S., Grüning, C., Faloon, K., Beddows, D., Harrison, R., Monahan, C., Jennings, S. G., O'Dowd, C. D., Marinoni, A., Horn, H.-G., Keck, L., Jiang, J., Scheckman, J., McMurry, P. H., Deng, Z., Zhao, C. S., Moerman, M., Henzing, B., de Leeuw, G., Löschau, G., and Bastian, S.: Mobility particle size spectrometers: harmonization of technical standards and data structure to facilitate high quality long-term observations of atmospheric particle number size distributions, *Atmospheric Meas. Tech.*, 5,

735 657–685, <https://doi.org/10.5194/amt-5-657-2012>, 2012.

Zelenyuk, A., Cai, Y., and Imre, D.: From Agglomerates of Spheres to Irregularly Shaped Particles: Determination of Dynamic Shape Factors from Measurements of Mobility and Vacuum Aerodynamic Diameters, *Aerosol Sci. Technol.*, 40, 197–217, <https://doi.org/10.1080/02786820500529406>, 2006.